# CALIBRATION OF THE NOL LARGE SCALE GAP TEST; HUGONIOT DATA FOR POLYMETHYL METHACRYLATE

J. O. Erkman, et al

Naval Ordnance Laboratory
White Oak, Maryland

4 April 1973

# CALIBRATION OF THE NOL LARGE SCALE GAP TEST; HUGONIOT DATA FOR POLYMETHYL METHACRYLATE

4 APRIL 1973



NOL

NAVAL ORDNANCE LABORATORY, WHITE OAK, SILVER SPRING, MARYLAND



NOLTR 73-15

UNCLASSIFIED
Security Classification

**DOCUMENT CONTROL DATA - R & D**

(Security classification of title, body of abstract and indexing annotation must be entered when the overall report is classified)

| | |
|---|---|
| 1 ORIGINATING ACTIVITY (Corporate author)<br>NAVAL ORDNANCE LABORATORY<br>WHITE OAK, SILVER SPRING, MD 20910 | 2a. REPORT SECURITY CLASSIFICATION<br>UNCLASSIFIED<br>2b. GROUP |

3 REPORT TITLE
Calibration of the NOL Large Scale Gap Test; Hugoniot Data for Polymethyl Methacrylate

4 DESCRIPTIVE NOTES (Type of report and inclusive dates)

5 AUTHOR(S) (First name, middle initial, last name)
J. O. ERKMAN, D. J. EDWARDS, A. R. CLAIRMONT, JR., AND DONNA PRICE

| | | |
|---|---|---|
| 6 REPORT DATE<br>4 April 1973 | 7a. TOTAL NO OF PAGES<br>21 | 7b. NO OF REFS<br>18 |
| 8a CONTRACT OR GRANT NO<br>N/A<br>b PROJECT NO<br>c<br>d | 9a. ORIGINATOR'S REPORT NUMBER(S)<br>NOLTR 73-15<br>9b. OTHER REPORT NO(S) (Any other numbers that may be assigned this report) | |

10 DISTRIBUTION STATEMENT
APPROVED FOR PUBLIC RELEASE; DISTRIBUTION UNLIMITED.

| | |
|---|---|
| 11 SUPPLEMENTARY NOTES | 12 SPONSORING MILITARY ACTIVITY<br>Naval Material Command<br>Washington, D. C. 20360 |

13 ABSTRACT

More accurate calibrations of peak pressure (P) vs gap length (x) are presented for the NOL large scale gap test for both pentolite and tetryl donor charges. These calibrations are derived from particle velocity and shock velocity measurements in the polymethyl methacrylate (PMMA) attenuator. Particle velocities are recorded by the electromagnetic velocity gage; shock velocities are determined from streak camera records of the progress of shocks through the attenuators. The new calibrations will allow direct comparison on a peak pressure basis of the results of tests performed in the past, mostly with tetryl donor charges, and those which have been performed recently with pentolite donor charges All future gap tests will use pentolite donor charges.

As indicated above, we measured both shock velocity (U) and particle velocity (u). However, the Hugoniot of PMMA was selected by comparing these U-u data with the low pressure U-u data recently published by Sandia Corporation; the experimental design and accuracy of the latter work is superior to those of the gap test for Hugoniot determinations. The Hugoniot so obtained was used in conjunction with our u-x data to produce the desired calibration curves (P-x).

The new tetryl calibration has about 20% greater P at 140 cards than that of the previously published calibration. This new curve does not cross the old curve; therefore the relative ranking of explosives by gap sensitivity will not be changed by the use of the new relation.

DD FORM 1 NOV 1473 (PAGE 1)
S/N 0101-807-6801

UNCLASSIFIED
Security Classification

Security Classification

| KEY WORDS | LINK A | | LINK B | | LINK C | |
|---|---|---|---|---|---|---|
| | ROLE | WT | ROLE | WT | ROLE | WT |
| Shock Sensitivity | | | | | | |
| Gap Test | | | | | | |
| Explosive | | | | | | |
| Electromagnetic Velocity Gage | | | | | | |
| Plexiglas Hugoniot | | | | | | |
| Pentolite Donor | | | | | | |
| Tetryl Donor | | | | | | |
| Calibration | | | | | | |

DD FORM 1 NOV 1473 (BACK)
(PAGE 2)



UNCLASSIFIED
Security Classification

# CALIBRATION OF THE NOL LARGE SCALE GAP TEST; HUGONIOT DATA FOR POLYMETHYL METHACRYLATE

Prepared by:

J. O. Erkman, D. J. Edwards, A. R. Clairmont, Jr., and Donna Price

ABSTRACT: More accurate calibrations of peak pressure (P) vs gap length (x) are presented for the NOL large scale gap test for both pentolite and tetryl donor charges. These calibrations are derived from particle velocity and shock velocity measurements in the polymethyl methacrylate (PMMA) attenuator. Particle velocities are recorded by the electromagnetic velocity gage; shock velocities are determined from streak camera records of the progress of shocks through the attenuators. The new calibrations will allow direct comparison on a peak pressure basis of the results of tests performed in the past, mostly with tetryl donor charges, and those which have been performed recently with pentolite donor charges. All future gap tests will use pentolite donor charges.

As indicated above, we measured both shock velocity (U) and particle velocity (u). However, the Hugoniot of PMMA was selected by comparing these U-u data with low pressure U-u data recently published by Sandia Corporation; the experimental design and accuracy of the latter work is superior to those of the gap test for Hugoniot determination. The Hugoniot so obtained was used in conjunction with our u-x data to produce the desired calibration curves (P-x).

The new tetryl calibration has about 20% greater P at 140 cards than that of the previously published calibration. This is largely due to the much improved definition of the wave interaction in the attenuator at a distance of about 35 mm from the donor charge which results in an abrupt change in the slope of the u-x curve at that distance. This phenomenon is also observed in the streak camera records of the progress of shocks through the attenuator; the shock velocity vs distance curve derived from the records has a hump at 30-40 mm from the donor. The new calibration curve does not cross the old curve; therefore the relative ranking of explosives by gap sensitivity will not be changed by the use of the new relation.

The pentolite calibration curve gives larger values of P than does the tetryl calibration for x < 200 cards (50 mm). The difference is not significant experimentally because it is the order of magnitude of errors in both calibrations. Excluding the nominal range (x < 10 mm), the greatest difference is 2.6 kbar, or 7%, at 140-150 cards. For x > 200 cards, the two new calibrations are coincident.

Approved by:

JOSEPH DACONS, Acting Chief
Advanced Chemistry Division
Chemistry Research Department
NAVAL ORDNANCE LABORATORY
White Oak, Silver Spring, Maryland

NOLTR 73-15 4 April 1973

CALIBRATION OF THE NOL LARGE SCALE GAP TEST; HUGONIOT DATA FOR POLYMETHYL METHACRYLATE

The work described in this report was carried out under Task IR-59, Transition From Deflagration to Detonation, of NOL's Independent Research Program. The results are more accurate calibrations of the NOL large scale gap test for both tetryl and pentolite donor charges and a more accurate representation of the Hugoniot of PMMA. These results are of importance to the study of the shock sensitivity of explosives and propellants.

The authors wish to thank Mr. Stanley Gerner of the Bureau of Standards Optical Shop for his careful preparation of the PMMA cylinders for the shock velocity experiments.

ROBERT WILLIAMSON II
Captain, USN
Commander

ALBERT LIGHTBODY
By direction

CONTENTS



ILLUSTRATIONS

ILLUSTRATIONS (Cont.)



TABLES

# 1. INTRODUCTION

Two major and related objectives of this work are (a) to recalibrate the large scale gap test (LSGT) and (b) to select the best Hugoniot for polymethyl methacrylate (PMMA). A calibration (or a check of it) has to be made whenever a new lot of donor pellets is received. The present recalibration differs from such a routine check in that we are able for the first time to measure particle velocity directly and accurately (to ± 0.03 mm/ sec), and also because exact data (shock velocity, U, vs particle velocity, u) defining the Hugoniot of PMMA in the lower pressure range have been published only recently. Use of the new method, the new data, and improved optics and data reduction for determinations of U showed that both of our old calibrations[1] (tetryl and pentolite loaded PMMA) are less accurate than is justified by our present improved capabilities.

An accurate Hugoniot (shock velocity, U, vs particle velocity, u) for PMMA, the attenuator in the LSGT, is necessary to carry out a calibration by measuring only one of these variables as a function of attenuator thickness. Unfortunately, the Hugoniots proposed for PMMA are legion. Heretofor we have used our U-u values[1] derived from indirect measurements; those values were definitely less precise than our present ones. Publication of exact data in the lower pressure region, in combination with our own improved measurements of U and u, allows us to construct what we consider an accurate PMMA Hugoniot over the pressure range of the gap test.

# 2. METHODS FOR CALIBRATING GAP TESTS

This section gives a brief review of methods that have been used, or could be used, to calibrate gap tests. For some of these, an analysis is given of the error inherent in the method. One method is direct: manganin pressure gages could be used.[2] By doing experiments in which the gage was at different distances from the explosive, a P vs x relation would result. This direct method is seldom used, possibly because it is still relatively new. For this reason, no error analysis will be given here.

Most gap calibrations are based on the well known relation between pressure, P, shock velocity, U, the particle velocity, u, and the density, $\rho_o$,

$$P = \rho_o U u \qquad (1)$$

and

$$U = a + b\,u \tag{2}$$

where a and b are known constants of the gap material. The linear relation between U and u is one way of describing the Hugoniot of a material. For many materials, the linear relation holds over a wide range, starting at low pressure. However the Hugoniot of PMMA is noticeably curved at low pressure as will be discussed in a later section. The linear relation will be useful in considering the errors inherent in the methods discussed in the following.

If the Hugoniot is known, measuring U as a function of x gives a pressure calibration. This is the usual method of calibrating gap tests. The dependency of shock velocity on distance is obtained by differentiating streak camera records which give shock position vs time. The errors involved in this method can be estimated by combining Equations (1) and (2) and taking the total differential, $\Delta P$, and dividing by P;

$$\frac{\Delta P}{P} = \left(\frac{2U-a}{U-a}\right)\frac{\Delta U}{U} + \left(\frac{a}{U-a}\right)\frac{\Delta a}{a} + \frac{\Delta b}{b} \tag{3}$$

Signs on the last two terms have been changed from negative to positive. Notice that the coefficients of the first term is greater than 1.0. This means, of course, that the error in P is greater than that in U; in this sense, the calculation of P amplifies the error in U. Also, when U→a, this amplification is more serious so that the accuracy of the calibration at low pressure is worse than that at high pressure.

Shock velocity, U, is obtained by either a numerical or graphical differentiation of time-distance data, usually from streak camera records. Accuracy of these methods is difficult to estimate; it is generally conceded that differentiation of numerical data is not a highly accurate process. Our data are probably somewhat inaccurate also, so we have two sources of error in our values of U. We can obtain some feel for the problem by taking the difference between values of U from two different sets of data -- see Section 3. This difference is a maximum of 0.12 for U ≈ 4.0 mm/μsec, or about 3%. Hence our error in P from this source is 11% because the coefficient in Equation (3) is

$$(2 \times 4.0 - 2.5)/(4.0 - 2.5) = 3.7$$

The range of U is from 6.0 to 3.0 mm/μsec in our calibration. A 3% error in U then contributes from 8% to 21% to the error in P over this range. This is the chief fault of this method. Accurate values of U are very difficult to obtain and the error in P, on a relative, or percentage basis is even larger than that in U. In the above it was assumed that U could be measured to the same percentage error over the range 6.0 to 3.0. Had we assumed that the absolute error is 0.12 over the range, our percent error would be 28% in P at the lower value of U.

Equation (3) shows that the error in a is also amplified, while that of b is only added in the accumulation. These constants are usually determined by a least squares method. Values of a and b, and in most cases, their respective quadratic mean errors (QME's) are as follows for some representative data.

| Source of data | a | b |
|---|---|---|
| High pressure data of Price and Liddiard[3] | 2.554±0.017 | 1.618±0.019 |
| 70 mm camera data of Liddiard and Price[4] | 2.554±0.015 | 1.693±0.016 |
| Hauver and Melani[5] | 2.68 | 1.61 |

For a given set of data, the constants are well determined -- their QME's are small. The variation in the values of a is about 0.13, or 5% of the average value of a. The variation in b is also about 5%. These, when added to the above estimate for the contribution of the error in U, give a range in the variation of P of from 18% to 31% for U varying from 6 to 3 mm/μsec. These possible errors are greater than desirable -- other methods should be examined in the hope of obtaining a more accurate calibration.

An alternate method is to measure the particle velocity as a function of x. Again, it is assumed that the Hugoniot is known. For an analysis of the error of this method, it is also assumed that the U,u relation is linear. Combining Equations (1) and (2) as before and taking the total differential gives

$$\frac{\Delta P}{P} = \left(1 + \frac{bu}{U}\right)\frac{\Delta u}{u} + \frac{a}{u}\,\frac{\Delta a}{a} + \frac{ub}{U}\,\frac{\Delta b}{b} \qquad (4)$$

where it has been convenient to retain U in place of the quantity (a + bu). Here none of the coefficients behave badly. That is, none of them tend to increase greatly, which is an advantage of this

method. The coefficients are all functions of u, so it is of interest to tabulate them over a range of values of u. These are given in Table 1, for which U = 2.576 + 1.602 u. Note that the first and third coefficients increase with u. These do not increase catastrophically, however. Assume that $\Delta u = 0.01$, and that $\Delta a/a = \Delta b/b = 0.05$, or 5%. Note that over the range $0.1 \leq u \leq 1.8$, the error in u ranges from 10% to 0.6%. The errors in P (in %) are given in Table 1 under the heading $E_1$. These range from 16% down to 5.7% while U varies from 2.74 to 6.1. This is considerably better than the results for the preceding case.

The values assumed for the errors in u, a and b may not be realistic; smaller values could have been used for the errors in the constants, for example. The values which were used are consistent with those used in the previous example, however. In the case of u, the error may be larger than that assumed. In Section 4 it will be shown that replicate shots give a spread as great as 0.03 and 0.04 mm/μsec. These values would increase the estimated error in P considerably. We can hope that the curve we draw through the points on a plot of u vs x gives values of u which are more accurate than 0.04 in absolute value over most of the range. That is, the smoothing which results when a curve is fitted to the points reduces the error in u at individual values of x.

A disadvantage of measuring u vs x for gap calibration is that many experiments must be done to establish the relation. The relation turned out to be somewhat more complicated than was anticipated, as will be pointed out in Section 4. In contrast, the method based on measuring U, requires, in principle, only a single streak camera record for the calibration. The work has rarely been this easy; it is found that each record gives a somewhat different curve, possibly due to variations in the experiment, as well as in reading and interpreting the record. Usually the average of several shots is used for a calibration. But far fewer shots are required than when particle velocity is measured.

Finally, both u and U can be measured as functions of x. Then the error in P is

$$\frac{\Delta P}{P} = \frac{\Delta u}{u} + \frac{\Delta U}{U} \qquad (5)$$

The error in P in % is given in the last column of Table 1, based on $\Delta u/u = 0.01$ and $\Delta U/U = 0.05$ (see preceding example). These errors, $E_2$ in Table 1, are comparable to those labeled $E_1$. We have the alternatives -- if the Hugoniot is well known, measuring u is sufficient. Otherwise, measure both u and U as functions of x. A variant of this latter method was used when free surface velocity was measured as a function of the gap length.[4] The calibration of this report is a variant also. We measure both u and U as functions of x, extract Hugoniot data from the measurements, then use the u vs x relation to obtain P vs x.

Table 1

Errors When Particle Velocities Are Measured

| u mm/μsec | U* mm/μsec | (1 + bu/U) | a/U | bu/U | $E_1$ % | $E_2$ % |
|---|---|---|---|---|---|---|
| 0.1 | 2.74 | 1.09 | 0.94 | 0.09 | 16.0 | 15.0 |
| 0.2 | 2.90 | 1.11 | 0.89 | 0.11 | 10.6 | 10.0 |
| 0.6 | 3.54 | 1.27 | 0.73 | 0.27 | 7.1 | 6.7 |
| 1.0 | 4.18 | 1.38 | 0.62 | 0.38 | 6.4 | 6.0 |
| 1.4 | 4.82 | 1.47 | 0.53 | 0.47 | 6.0 | 5.7 |
| 1.8 | 5.46 | 1.53 | 0.47 | 0.53 | 5.8 | 5.6 |
| 2.0 | 5.78 | 1.55 | 0.45 | 0.55 | 5.8 | 5.5 |
| 2.3 | 6.10 | 1.58 | 0.42 | 0.58 | 5.7 | 5.4 |

*U = 2.576 + 1.602 u.

The method discussed above gives the Hugoniot of the gap material. As will be shown in Section 5, the resulting Hugoniot of PMMA has some peculiar features which we attribute to errors in our measurements. Examining this relation has, hopefully, helped us to reduce some of the errors. The errors are probably caused, at least in part, by the rapid attenuation of the shock wave, and the interaction of relief waves from the periphery of the cylinder. In work with the primary objective of Hugoniot measurements, both of these complications are excluded from the experiments by proper design. Hence it is advantageous to use a material in the gap which has already been characterized in careful studies. Then the preferred method for calibrating the gap test would be to measure the particle velocity as a function of x, using the electromagnetic gage as has been done in this work.

## 3. SHOCK VELOCITY IN PMMA SHOCKED BY PENTOLITE

This section gives an account of the measurement of the shock velocity in the PMMA attenuator of the LSGT when pentolite* is used as the donor explosive. In the past, most gap tests have been calibrated by the procedure described in the remainder of this section. That is, the shock velocity was determined as a function of the length of the attenuator; then the Hugoniot equation of state of the attenuating material was used to convert shock velocities to pressures. Now, we are not so dependent on the shock velocity measurements; independent measurements of particle velocity have also been made. Some of the results of this section will be used in conjunction with particle velocity measurements to establish a better Hugoniot for PMMA, see Section 5.

Experimental. The experimental arrangement for measuring shock velocity in the PMMA attenuator is given by Liddiard and Price[4] and others. Essentially the same arrangement was used in this work. The exception is that no baffle was used between the pentolite and the PMMA. The PMMA was prepared so that the distance between flats, see Figure 1, was 50.8 mm or slightly greater. This arrangement seems to be adequate, at least in most cases, to prevent the detonation product gases from interfering with photographing the shock front.

---

*The pentolite pellets were obtained from NAD, Crane, Indiana. They replace graphited tetryl pellets, $\rho_o$ = 1.51 g/cc, which are no longer available. The pentolite pellets are identified as Federal Stock No. 1375-991-8891. They are described in BUWEPS drawing No. 210 8395, "Pellet, Pentolite, Donor, Standard", and are pressed to a density of 1.56 g/cc as per "Advisory Process For The Pressing Of Standard Donor Pentolite Pellets", NAWEPS OD 29872, 16 June, 1964. See the Appendix for comments on the uniformity of the dimensions of the pellets.

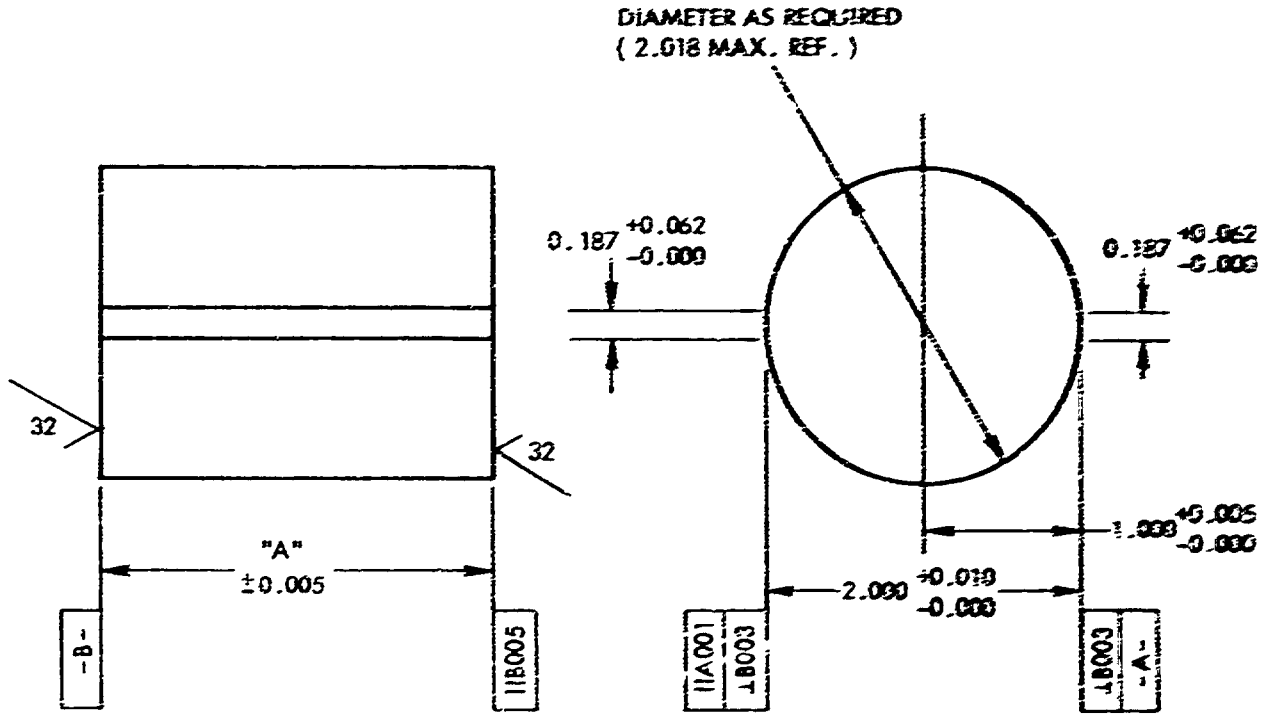


| PIECE NO. | "A" |
|---|---|
| 1 | 2.500 |
| 2 | 4.500 |

NOTE:
1. 63/ ALL OVER EXCEPT AS NOTED.
2. REMOVE BURRS AND SHARP EDGES 0.031 -R MAX.
3. THE TWO 0.187 WIDE FLATS ARE TO BE GROUND AND OPTICALLY POLISHED TO WITHIN 2 WAVES/INCH OF LENGTH.
4. BOTH FLATS SHALL BE SCRATCH FREE AND TRANSPARENT.

FIG. 1 MACHINE DRAWING FOR PREPARATION OF CYLINDERS FOR LSGT CALIBRATION

Specifications for preparing the attenuation cylinders are given in Figure 1. The cylinders were machined and polished in the Optics Shop of the National Bureau of Standards starting with 63 mm (2.5 inch) diameter cast rod. They were free from the optical distortion reported on cylinders used in earlier work. That is, the flats were not rounded during the polishing operation to form a barrel lens. Also, the ends of the flats were kept parallel to the axis of the cylinders.

Other system improvements suggested in reference (6) were (a) use of a better lens in the light source, (b) glass window in the camera port, (c) parallel light through the sample, (d) better focusing of the camera and (e) restricting the length being observed. These improvements will be discussed in turn.

Light for observing the shock front in the PMMA is obtained by discharging a capacitor through a bridgewire. The light is collimated by using a simple lens. In the past, these have been 152 mm diameter, 356 mm focal length plano convex lenses (the same as or similar to Stock Number 1189 in the Catalog of Edmund Scientific Company). These lenses show definite striations when observed obliquely in reflected light. Lenses used in this work were 91 mm in diameter and had a focal length of 215 mm. These were obtained from A. Jaegers as Stock Number 29A2567. Although these are not high quality lenses, they do not show the striations mentioned above, and are therefore considerably better than those used previously.

Glass windows were used in the camera port for the shots reported here. These windows were cut from "Select" quality plate glass 1.0 inch thick. Use of glass windows gives demonstrably better still photographs in the streak camera. The improvement is assumed to carry over to the photographing of dynamic events.

During shot setup, the light source and the collimating lens were arranged to give parallel light through the specimen. The reason for this arrangement was discussed in reference (6). The use of parallel light makes it impossible to photograph a 10 cm length of the specimen because the aperture in the camera port is only 8.8 cm in diameter. The field of view was restricted to about 60 mm. For two shots, the section observed was between 0 and 60 mm from the loaded end of the specimen. For the second pair of shots, the section between about 40 and 110 mm from the loaded end was observed. As noted in reference (6), this arrangement gives more nearly optimal recording on the film. That is, the slope of the trace on the film was closer to unity than in earlier work. The camera writing speed was 4.0 mm/μsec; a speed of 5.0 mm/μsec would have improved the records for the first pair of shots ($x \leq 60$ mm).

The camera was focused on the plane containing the axis of symmetry of the PMMA cylinder. The reason for this is also given in reference (6).

Data Reduction. The streak camera records give the position of the shock front, x, as a function of time, T. These records are "read" on a Universal Telereader as described previously.[6,7] There results a set of digitized data giving pairs of values of x and T. These data were smoothed and differentiated using the method described in reference (6). This method was called the local smoothing and differentiation (lsd) method. The first step of the method consists of getting a "smoothed" value of T for a particular value of x by least square fitting a quadratic to the four neighboring points. The quadratic is then solved for the new value of the time, $T_s$. Each point in the set of data is treated similarly to generate a new set, $T_s$ vs x.

The $x, T_s$ set of data is differentiated by fitting a quadratic to three points. This gives an exact fit (except for round off error) to the points. The shock velocity is determined from the derivative of the quadratic at the second of the three points being considered. There result tables of x, $T_s$ and $U^{-1}$. Finally, the values of $U^{-1}$ are smoothed in the same manner that was used for smoothing values of time except that a straight line, rather than a quadratic, is used to fit five points instead of four.

In the numerical work, x is used as the independent variable for reasons given in reference (6). Hence the derivative mentioned above is the reciprocal of the shock velocity, i.e., dT/dx.

Results of the first trial at reducing the data for the four shots are given in Figure 2 and Tables 2 through 5. In the figure, the shock velocity, U, is given as a function of the distance, x. In the tables, the first and second columns give T and x, respectively in units of "counts" on the Telereader; in the next two columns they are given in μsec and mm respectively. The fifth column gives the shock velocity in mm/μsec as evaluated by processes discussed above. First divided differences in x and T (here T is used as the independent variable) are given in the last column of each table. Divided differences are useful in evaluating the quality of the data in the following discussion.

For Shots 865 and 867, the camera recorded shock travel from x = 0.0 to about 60 mm. Results for Shot 865 appear to be good (comparable with the better shots in reference (6), for example). This judgment is based on observing the behavior of U in Figure 2, and on the divided differences in Table 2. These latter generally decrease with increasing x as they should. There are "irregularities" in the differences; the sixth value is greater than the preceding value so that $\Delta U/\Delta x > 0.0$. This would not happen if each pair of values of x and T lay on a smooth curve. (Note: The first entry in Column 6 has no meaning). Continuing the examination, the 13th is greater than the two preceding it. These irregularities in the data did not defeat the scheme used to obtain the values of U -- note the results in Column 5, Table 2 and in Figure 2.

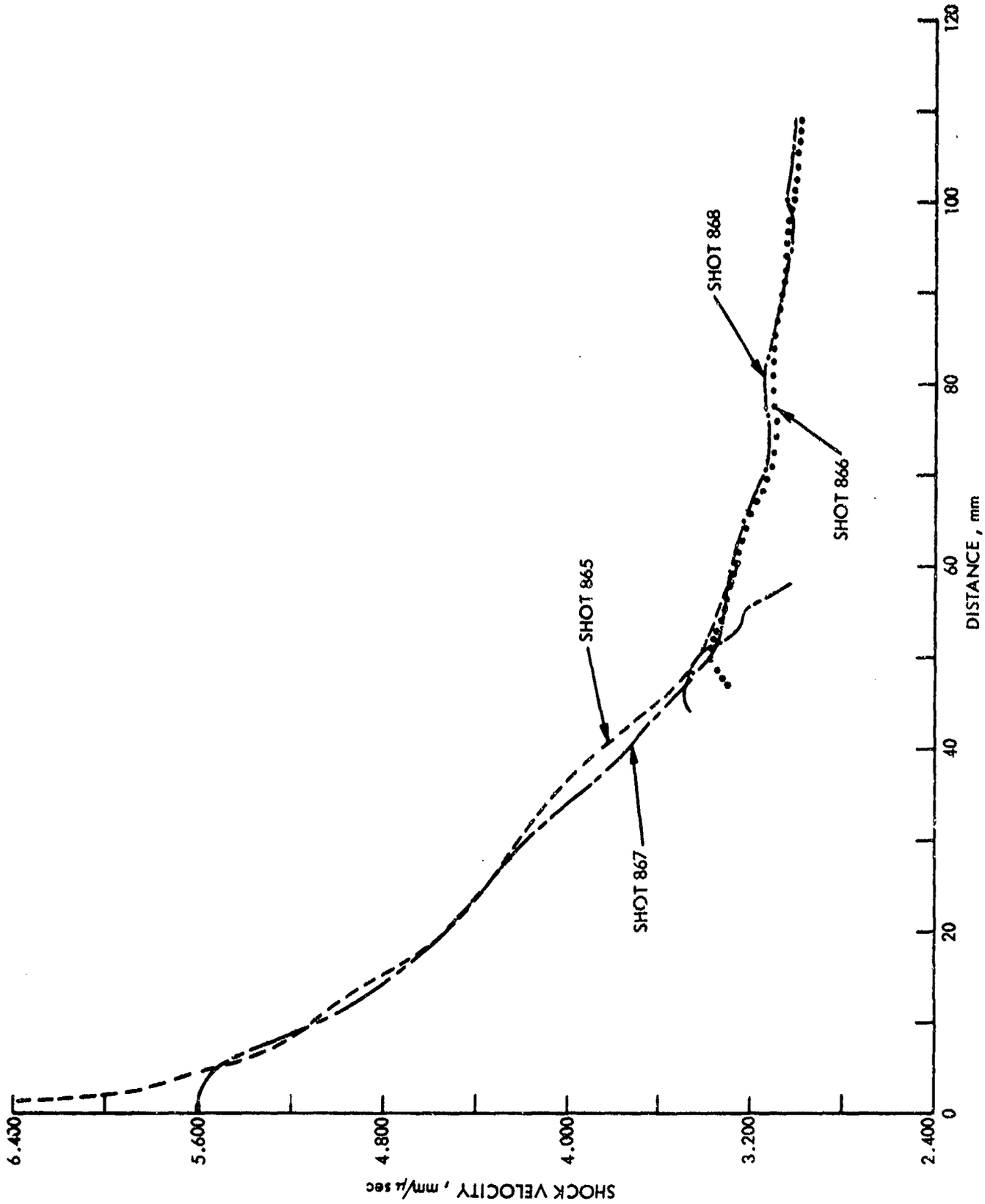


FIG. 2 SHOCK VELOCITY VS DISTANCE (FIRST TRIAL OF DATA REDUCTION PROCESS)

TABLE 2

DATA AND RESULTS FOR SHOT 865

| TIME COUNTS | DISTANCE COUNTS | TIME μSEC | DISTANCE MM | U MM/μSEC | DIFF. MM/μSEC |
|---|---|---|---|---|---|
| 0.0 | 16.0 | .000 | .255 | 8.783 | 0.000 |
| 10.0 | 39.0 | .038 | .622 | 7.664 | 9.769 |
| 19.0 | 55.0 | .072 | .878 | 7.041 | 7.568 |
| 35.0 | 76.0 | .131 | 1.213 | 6.511 | 5.599 |
| 59.0 | 106.0 | .221 | 1.691 | 6.130 | 5.334 |
| 90.0 | 153.0 | .337 | 2.441 | 5.880 | 6.462 |
| 136.0 | 214.0 | .509 | 3.414 | 5.764 | 5.657 |
| 174.0 | 267.0 | .651 | 4.260 | 5.665 | 5.948 |
| 219.0 | 327.0 | .820 | 5.217 | 5.521 | 5.687 |
| 268.0 | 390.0 | 1.003 | 6.222 | 5.379 | 5.485 |
| 316.0 | 447.0 | 1.182 | 7.132 | 5.292 | 5.068 |
| 371.0 | 512.0 | 1.388 | 8.169 | 5.212 | 5.044 |
| 455.0 | 617.0 | 1.702 | 9.844 | 5.127 | 5.334 |
| 546.0 | 725.0 | 2.042 | 11.567 | 5.031 | 5.066 |
| 643.0 | 844.0 | 2.405 | 13.466 | 4.920 | 5.235 |
| 771.0 | 988.0 | 2.883 | 15.763 | 4.758 | 4.803 |
| 905.0 | 1128.0 | 3.384 | 17.997 | 4.617 | 4.462 |
| 999.0 | 1233.0 | 3.735 | 19.672 | 4.529 | 4.769 |
| 1122.0 | 1362.0 | 4.195 | 21.730 | 4.445 | 4.479 |
| 1309.0 | 1549.0 | 4.893 | 24.714 | 4.354 | 4.272 |
| 1459.0 | 1703.0 | 5.453 | 27.171 | 4.284 | 4.385 |
| 1626.0 | 1870.0 | 6.077 | 29.835 | 4.208 | 4.272 |
| 1812.0 | 2052.0 | 6.772 | 32.739 | 4.119 | 4.180 |
| 1961.0 | 2195.0 | 7.328 | 35.021 | 4.044 | 4.100 |
| 2131.0 | 2356.0 | 7.963 | 37.589 | 3.949 | 4.046 |
| 2276.0 | 2486.0 | 8.504 | 39.664 | 3.860 | 3.832 |
| 2411.0 | 2609.0 | 9.008 | 41.626 | 3.772 | 3.893 |
| 2586.0 | 2764.0 | 9.662 | 44.099 | 3.651 | 3.785 |
| 2715.0 | 2872.0 | 10.143 | 45.812 | 3.571 | 3.579 |
| 2854.0 | 2984.0 | 10.662 | 47.609 | 3.495 | 3.445 |
| 2974.0 | 3084.0 | 11.110 | 49.205 | 3.441 | 3.562 |
| 3103.0 | 3184.0 | 11.591 | 50.800 | 3.401 | 3.315 |
| 3123.0 | 3197.0 | 11.666 | 51.007 | 3.394 | 2.781 |
| 3222.0 | 3284.0 | 12.035 | 52.395 | 3.371 | 3.756 |
| 3363.0 | 3386.0 | 12.561 | 54.023 | 3.350 | 3.094 |
| 3479.0 | 3480.0 | 12.994 | 55.523 | 3.331 | 3.464 |
| 3600.0 | 3574.0 | 13.446 | 57.022 | 3.312 | 3.322 |
| 3715.0 | 3662.0 | 13.875 | 58.426 | 3.289 | 3.272 |
| 3790.0 | 3720.0 | 14.155 | 59.352 | 3.274 | 3.307 |
| 3867.0 | 3779.0 | 14.442 | 60.293 | 3.258 | 3.276 |

Shot 867 gave results which are inferior to those of 865, see Table 3 and Figure 2. Values of U are too small for $x < 5$ mm, and for $x > 47$ mm. This "badness" is in the digital data and presumably in the streak camera trace itself -- it is not an artifact of the numerical operations. This conclusion is substantiated by the behavior of the differences in Table 3. Values of the differences do not decrease with x smoothly. The same situation is observed between 49.6 and 51.3 mm, and near the end of the table.

For Shot 866 (x varies from 47 to 109 mm), U increases with x for $47 \leq x \leq 51$ and for $75 \leq x \leq 82$, see Table 4. The first 3 values of the differences bear out the first observation. The increase of U with x near 80 mm may be due to the data which resulted in the value 3.211 for the difference at 80.3 mm. For this shot also, there are irregularities in the data which are not due to the numerical methods. Unfortunately, the numerical methods cannot remove the irregularities.

Results for Shot 868 (Table 5) are much the same as those of Shot 866 discussed immediately above. There must be a reproducible cause for the peculiar behavior observed at the beginning of each of these records. It was thought that this behavior was due to inaccurate flats near the ends of the PMMA cylinders. More care in preparing these flats has not eliminated the trouble. In the following, these irregular results (at the beginning of the records, and the oscillatory behavior later in the records of 866 and 868, see Figure 2) are treated as errors, and the deviations from the expected results are eliminated, or at least, smoothed.

Defects in the results could possibly be reduced by using more forceful smoothing of the x,T and the $x,U^{-1}$ data using graphical or numerical methods. It was done by removing those data which appear to be the chief causes of the trouble. This is a subjective process; it was guided by examining the behavior of U and the divided differences in Figure 2 and in Tables 2 through 5. Data eliminated are the following:

| Shot No. | Data Removed For Values of x of |
|---|---|
| 865 | none |
| 867 | 0.0 through 4.54 mm<br>49.6 through 52.1 mm<br>55.7 through 57.7 mm |
| 866 | 47.1 through 49.9 mm |
| 868 | 44.2 through 47.9 mm |

The revised sets of data were treated in the same way as the originals, see above. Results, which are shown in Figure 3 are less

TABLE 3

DATA AND RESULTS FOR SHOT 867

| TIME COUNTS | DISTANCE COUNTS | TIME μSEC | DISTANCE MM | U MM/μSEC | DIFF. MM/μSEC |
|---|---|---|---|---|---|
| 0.0 | 0.0 | 0.000 | 0.000 | 5.618 | 0.000 |
| 23.0 | 43.0 | .086 | .680 | 5.610 | 7.912 |
| 66.0 | 88.0 | .246 | 1.392 | 5.601 | 4.439 |
| 107.0 | 145.0 | .399 | 2.294 | 5.596 | 5.892 |
| 155.0 | 209.0 | .579 | 3.307 | 5.573 | 5.651 |
| 214.0 | 287.0 | .799 | 4.541 | 5.527 | 5.604 |
| 276.0 | 368.0 | 1.030 | 5.822 | 5.448 | 5.538 |
| 330.0 | 440.0 | 1.232 | 6.961 | 5.358 | 5.651 |
| 405.0 | 531.0 | 1.512 | 8.401 | 5.219 | 5.144 |
| 488.0 | 632.0 | 1.821 | 9.999 | 5.079 | 5.159 |
| 551.0 | 707.0 | 2.056 | 11.185 | 4.984 | 5.048 |
| 658.0 | 828.0 | 2.456 | 13.099 | 4.855 | 4.796 |
| 733.0 | 916.0 | 2.735 | 14.492 | 4.773 | 4.975 |
| 882.0 | 1080.0 | 3.291 | 17.086 | 4.641 | 4.668 |
| 1045.0 | 1256.0 | 3.899 | 19.871 | 4.519 | 4.580 |
| 1205.0 | 1419.0 | 4.496 | 22.449 | 4.420 | 4.322 |
| 1335.0 | 1556.0 | 4.981 | 24.617 | 4.345 | 4.470 |
| 1446.0 | 1670.0 | 5.395 | 26.420 | 4.290 | 4.357 |
| 1564.0 | 1788.0 | 5.835 | 28.287 | 4.234 | 4.242 |
| 1682.0 | 1904.0 | 6.275 | 30.122 | 4.168 | 4.171 |
| 1799.0 | 2018.0 | 6.711 | 31.926 | 4.091 | 4.134 |
| 1905.0 | 2122.0 | 7.106 | 33.571 | 4.010 | 4.163 |
| 2014.0 | 2227.0 | 7.513 | 35.233 | 3.931 | 4.087 |
| 2153.0 | 2349.0 | 8.031 | 37.163 | 3.842 | 3.725 |
| 2309.0 | 2487.0 | 8.612 | 39.346 | 3.755 | 3.754 |
| 2457.0 | 2617.0 | 9.164 | 41.403 | 3.685 | 3.728 |
| 2571.0 | 2717.0 | 9.589 | 42.985 | 3.634 | 3.723 |
| 2666.0 | 2796.0 | 9.943 | 44.234 | 3.587 | 3.530 |
| 2774.0 | 2889.0 | 10.346 | 45.706 | 3.525 | 3.655 |
| 2913.0 | 3003.0 | 10.864 | 47.509 | 3.466 | 3.481 |
| 3014.0 | 3084.0 | 11.240 | 48.791 | 3.461 | 3.404 |
| 3083.0 | 3137.0 | 11.497 | 49.629 | 3.444 | 3.261 |
| 3126.0 | 3173.0 | 11.658 | 50.199 | 3.450 | 3.553 |
| 3162.0 | 3207.0 | 11.792 | 50.737 | 3.398 | 4.007 |
| 3174.0 | 3211.0 | 11.837 | 50.800 | 3.421 | 1.417 |
| 3207.0 | 3240.0 | 11.960 | 51.259 | 3.367 | 3.730 |
| 3277.0 | 3292.0 | 12.220 | 52.081 | 3.335 | 3.154 |
| 3343.0 | 3345.0 | 12.466 | 52.920 | 3.302 | 3.409 |
| 3415.0 | 3403.0 | 12.735 | 53.838 | 3.307 | 3.419 |
| 3499.0 | 3465.0 | 13.048 | 54.818 | 3.279 | 3.134 |
| 3566.0 | 3519.0 | 13.297 | 55.673 | 3.243 | 3.421 |
| 3625.0 | 3564.0 | 13.517 | 56.385 | 3.163 | 3.238 |
| 3688.0 | 3612.0 | 13.752 | 57.144 | 3.083 | 3.235 |
| 3742.0 | 3649.0 | 13.953 | 57.729 | 3.023 | 2.909 |

TABLE 4

DATA AND RESULTS FOR SHOT 866

| TIME COUNTS | DISTANCE COUNTS | TIME μSEC | DISTANCE MM | U MM/μSEC | DIFF. MM/μSEC |
|---|---|---|---|---|---|
| 0.0 | 0.0 | 0.000 | 47.130 | 3.291 | 0.000 |
| 65.0 | 50.0 | .242 | 47.921 | 3.314 | 3.262 |
| 153.0 | 119.0 | .571 | 49.013 | 3.346 | 3.325 |
| 224.0 | 177.0 | .836 | 49.930 | 3.362 | 3.464 |
| 311.0 | 248.0 | 1.160 | 51.054 | 3.364 | 3.461 |
| 387.0 | 307.0 | 1.444 | 51.987 | 3.353 | 3.292 |
| 474.0 | 375.0 | 1.768 | 53.063 | 3.334 | 3.315 |
| 588.0 | 464.0 | 2.194 | 54.471 | 3.312 | 3.311 |
| 724.0 | 572.0 | 2.701 | 56.179 | 3.293 | 3.368 |
| 888.0 | 695.0 | 3.313 | 58.125 | 3.277 | 3.181 |
| 1028.0 | 805.0 | 3.835 | 59.866 | 3.262 | 3.332 |
| 1160.0 | 906.0 | 4.327 | 61.463 | 3.246 | 3.245 |
| 1362.0 | 1062.0 | 5.081 | 63.931 | 3.216 | 3.275 |
| 1536.0 | 1192.0 | 5.730 | 65.988 | 3.184 | 3.169 |
| 1725.0 | 1333.0 | 6.435 | 68.219 | 3.145 | 3.164 |
| 1862.0 | 1438.0 | 6.946 | 69.880 | 3.116 | 3.251 |
| 2001.0 | 1535.0 | 7.464 | 71.415 | 3.094 | 2.961 |
| 2133.0 | 1632.0 | 7.956 | 72.949 | 3.080 | 3.117 |
| 2292.0 | 1747.0 | 8.549 | 74.769 | 3.077 | 3.068 |
| 2453.0 | 1863.0 | 9.150 | 76.604 | 3.082 | 3.056 |
| 2634.0 | 1992.0 | 9.825 | 78.645 | 3.092 | 3.023 |
| 2774.0 | 2098.0 | 10.347 | 80.322 | 3.097 | 3.211 |
| 2933.0 | 2214.0 | 10.940 | 82.157 | 3.097 | 3.095 |
| 3100.0 | 2337.0 | 11.563 | 84.103 | 3.088 | 3.124 |
| 3262.0 | 2453.0 | 12.167 | 85.938 | 3.077 | 3.038 |
| 3410.0 | 2560.0 | 12.719 | 87.631 | 3.066 | 3.067 |
| 3548.0 | 2661.0 | 13.234 | 89.229 | 3.056 | 3.105 |
| 3716.0 | 2781.0 | 13.860 | 91.127 | 3.045 | 3.030 |
| 3886.0 | 2902.0 | 14.494 | 93.041 | 3.036 | 3.019 |
| 4034.0 | 3011.0 | 15.046 | 94.766 | 3.029 | 3.124 |
| 4207.0 | 3130.0 | 15.692 | 96.649 | 3.022 | 2.918 |
| 4337.0 | 3223.0 | 16.176 | 98.120 | 3.017 | 3.035 |
| 4477.0 | 3325.0 | 16.699 | 99.734 | 3.010 | 3.091 |
| 4608.0 | 3418.0 | 17.187 | 101.205 | 3.004 | 3.012 |
| 4761.0 | 3524.0 | 17.758 | 102.882 | 2.996 | 2.939 |
| 4946.0 | 3654.0 | 18.448 | 104.939 | 2.983 | 2.981 |
| 5091.0 | 3757.0 | 18.998 | 106.568 | 2.980 | 3.013 |
| 5212.0 | 3842.0 | 19.440 | 107.913 | 2.978 | 2.980 |
| 5317.0 | 3915.0 | 19.831 | 109.068 | 2.977 | 2.950 |

TABLE 5

DATA AND RESULTS FOR SHOT 868

| TIME COUNTS | DISTANCE COUNTS | TIME μSEC | DISTANCE MM | U MM/μSEC | DIFF. MM/μSEC |
|---|---|---|---|---|---|
| 0.0 | 0.0 | 0.000 | 44.248 | 3.459 | 0.000 |
| 76.0 | 58.0 | .283 | 45.172 | 3.475 | 3.266 |
| 139.0 | 113.0 | .518 | 46.049 | 3.489 | 3.735 |
| 211.0 | 172.0 | .786 | 46.989 | 3.489 | 3.506 |
| 273.0 | 226.0 | 1.017 | 47.850 | 3.470 | 3.726 |
| 343.0 | 279.0 | 1.278 | 48.695 | 3.436 | 3.240 |
| 403.0 | 326.0 | 1.501 | 49.444 | 3.404 | 3.352 |
| 469.0 | 382.0 | 1.747 | 50.337 | 3.371 | 3.630 |
| 529.0 | 427.0 | 1.971 | 51.054 | 3.357 | 3.210 |
| 594.0 | 476.0 | 2.213 | 51.835 | 3.341 | 3.226 |
| 689.0 | 552.0 | 2.567 | 53.046 | 3.325 | 3.423 |
| 792.0 | 632.0 | 2.950 | 54.322 | 3.312 | 3.324 |
| 896.0 | 712.0 | 3.338 | 55.597 | 3.308 | 3.292 |
| 996.0 | 789.0 | 3.710 | 56.824 | 3.298 | 3.295 |
| 1111.0 | 875.0 | 4.139 | 58.195 | 3.288 | 3.200 |
| 1257.0 | 993.0 | 4.682 | 60.076 | 3.271 | 3.458 |
| 1389.0 | 1092.0 | 5.174 | 61.654 | 3.257 | 3.210 |
| 1541.0 | 1204.0 | 5.740 | 63.439 | 3.235 | 3.153 |
| 1707.0 | 1331.0 | 6.359 | 65.464 | 3.208 | 3.274 |
| 1868.0 | 1453.0 | 6.958 | 67.408 | 3.181 | 3.243 |
| 2013.0 | 1559.0 | 7.498 | 69.098 | 3.158 | 3.128 |
| 2155.0 | 1664.0 | 8.027 | 70.771 | 3.137 | 3.164 |
| 2282.0 | 1756.0 | 8.500 | 72.238 | 3.124 | 3.100 |
| 2402.0 | 1843.0 | 8.947 | 73.625 | 3.122 | 3.103 |
| 2519.0 | 1928.0 | 9.383 | 74.980 | 3.129 | 3.109 |
| 2647.0 | 2021.0 | 9.860 | 76.462 | 3.138 | 3.109 |
| 2816.0 | 2146.0 | 10.489 | 78.454 | 3.147 | 3.165 |
| 2996.0 | 2282.0 | 11.160 | 80.622 | 3.145 | 3.233 |
| 3138.0 | 2386.0 | 11.689 | 82.280 | 3.136 | 3.134 |
| 3326.0 | 2522.0 | 12.389 | 84.448 | 3.115 | 3.096 |
| 3457.0 | 2618.0 | 12.877 | 85.978 | 3.102 | 3.136 |
| 3580.0 | 2707.0 | 13.335 | 87.397 | 3.094 | 3.097 |
| 3688.0 | 2783.0 | 13.737 | 88.608 | 3.087 | 3.012 |
| 3850.0 | 2901.0 | 14.341 | 90.489 | 3.074 | 3.117 |
| 3948.0 | 2973.0 | 14.706 | 91.637 | 3.059 | 3.144 |
| 4088.0 | 3072.0 | 15.227 | 93.215 | 3.040 | 3.026 |
| 4205.0 | 3156.0 | 15.663 | 94.554 | 3.028 | 3.073 |
| 4377.0 | 3273.0 | 16.303 | 96.419 | 3.024 | 2.911 |
| 4528.0 | 3380.0 | 16.866 | 98.124 | 3.032 | 3.033 |
| 4668.0 | 3479.0 | 17.387 | 99.702 | 3.041 | 3.026 |
| 4775.0 | 3556.0 | 17.786 | 100.929 | 3.046 | 3.080 |
| 4921.0 | 3663.0 | 18.329 | 102.635 | 3.042 | 3.136 |
| 5041.0 | 3746.0 | 18.776 | 103.958 | 3.033 | 2.960 |
| 5174.0 | 3839.0 | 19.272 | 105.440 | 3.018 | 2.993 |
| 5267.0 | 3907.0 | 19.618 | 106.524 | 3.015 | 3.129 |
| 5323.0 | 3944.0 | 19.827 | 107.114 | 3.014 | 2.828 |
| 5380.0 | 3985.0 | 20.039 | 107.768 | 3.012 | 3.078 |

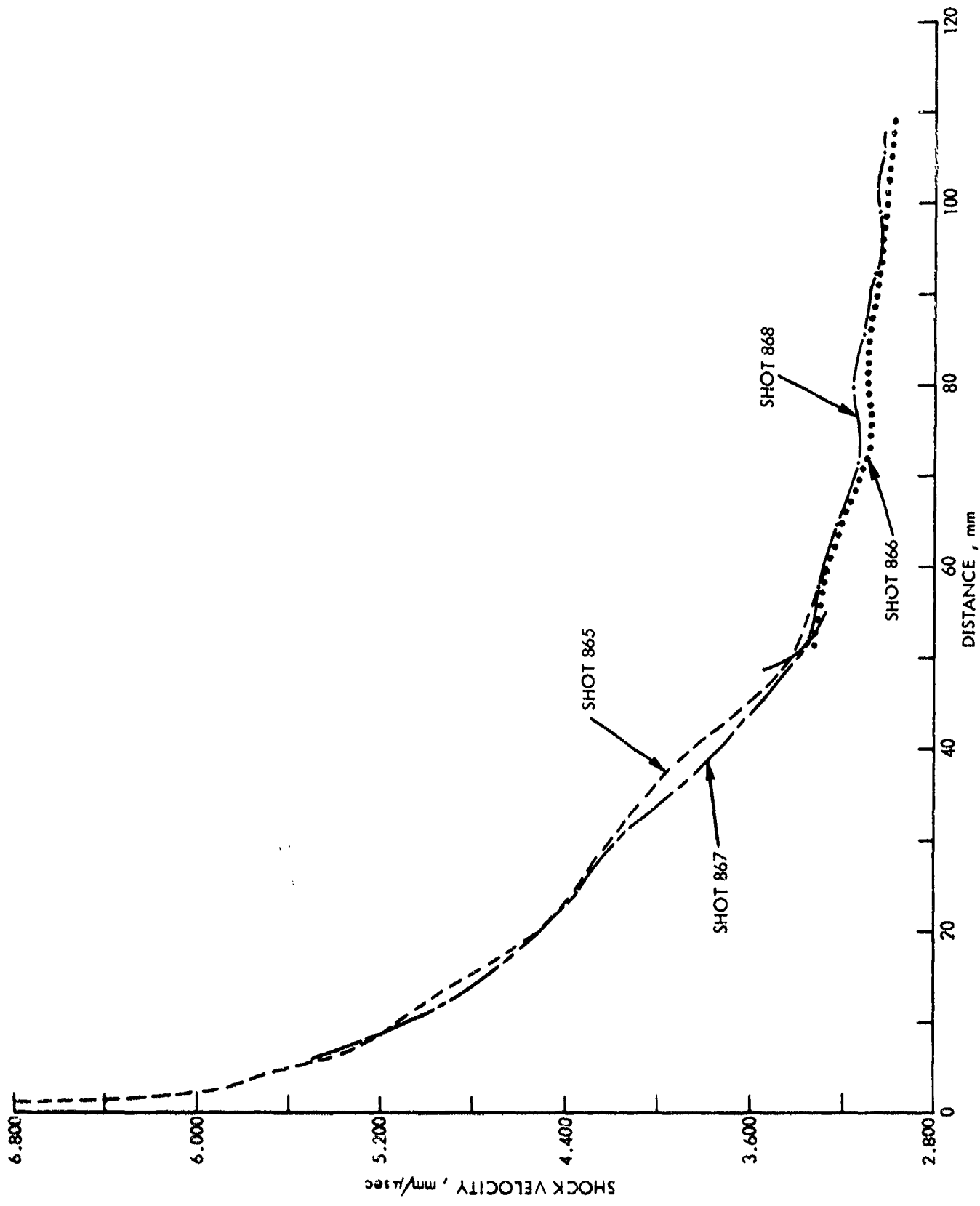


FIG. 3 SHOCK VELOCITY VS DISTANCE, FINAL RESULTS

erratic than those of Figure 2, as was expected. It is now necessary to combine all the data to give a single U vs x curve. This could be done graphically. Instead, a new set of results giving U at each mm in x for each shot are obtained by interpolating in the sets described above. Representative samples of these new sets are given in Table 6. The last column gives the differences in U for replicate shots; these tell something about the precision of the work. Note that these differences are greatest at 35 and 40 mm. This is the middle region of the "hump" previously observed in the U vs x curve.[4] It may be caused by interaction of rarefaction waves with the shock wave as has been mentioned above. This interaction apparently introduces some imprecision in our measurement of shock velocity.

Having values of U at equally spaced values of x for each pair of shots permits us to combine the results by averaging. Results for Shots 865 and 867 are averaged for $6 \leq x \leq 49$; Shots 866 and 868 are averaged for $50 \leq x \leq 105$. These new results are displayed in Figure 4.

The oscillations in the U,x curve of Figure 4 may or may not be real -- they are in the digital data, an observation borne out by the behavior of the divided differences. Here it is assumed that $\Delta U/\Delta x$ should be negative for all values of x. This condition can be forced on the results by fitting the averaged data (see above) with a cubic for $40 \leq x \leq 105$ mm. There results

$$U = 7.416 - 0.151\ x + 0.00179\ x^2 - 0.00000713\ x^3, \qquad (6)$$

which fits the data well, see the solid curve in Figure 4. The cubic has an inflection point (second derivative is zero) at 83.5 mm; it appears to cause no trouble. As desired, the first derivative remains negative over the interval of x in the data. For the final set of U,x data, the cubic is used for $45 \leq x \leq 105$ mm. For $8 \leq x \leq 45$ mm the averaged data are used -- these data are not fitted to a function. The use of these intervals insures that the two sets of data join smoothly. These data are all shown in Figure 4; a sampling is shown in Column 2 of Table 7.

If we relied on measurements of shock velocities for the calibration of the gap test for pentolite, we would have to obtain results in the interval $0.0 \leq x < 8$ mm. Because the shock velocity decreases with x very rapidly in this interval, it is much more difficult to measure than elsewhere. In the past, the Chapman-Jouguet variables have been evaluated for the explosive. Then a shock impedance method was used to calculate the pressure, particle velocity and shock velocity at the interface. This procedure ignores any effect of the finite reaction zone in the explosive. Here, we do not really need the shock velocities close to the explosive because we have particle velocity measurements instead (see next Section).

Table 6

SPREAD IN SHOCK VELOCITY BETWEEN SHOTS
(Interpolated Data)

| x | U, mm/usec | | | | |
|---|---|---|---|---|---|
| | Shot | Shot | Shot | Shot | Difference |
| mm | 865 | 867 | 866 | 868 | |
| 5 | 5.551 | | | | |
| 10 | 5.124 | 5.065 | | | 0.059 |
| 15 | 4.807 | 4.732 | | | 0.075 |
| 20 | 4.498 | 4.504 | | | 0.006 |
| 25 | 4.346 | 4.333 | | | 0.013 |
| 30 | 4.208 | 4.173 | | | 0.035 |
| 35 | 4.045 | 3.941 | | | 0.104 |
| 40 | 3.851 | 3.730 | | | 0.120 |
| 45 | 3.604 | 3.562 | | | 0.042 |
| 50 | 3.428 | 3.388 | | | 0.040 |
| 55 | | | 3.300 | 3.313 | 0.013 |
| 60 | | | 3.264 | 3.272 | 0.008 |
| 65 | | | 3.201 | 3.214 | 0.013 |
| 70 | | | 3.108 | 3.143 | 0.035 |
| 75 | | | 3.073 | 3.130 | 0.057 |
| 80 | | | 3.097 | 3.148 | 0.051 |
| 85 | | | 3.083 | 3.107 | 0.024 |
| 90 | | | 3.050 | 3.080 | 0.030 |
| 95 | | | 3.028 | 3.016 | 0.012 |
| 100 | | | 3.010 | 3.048 | 0.038 |

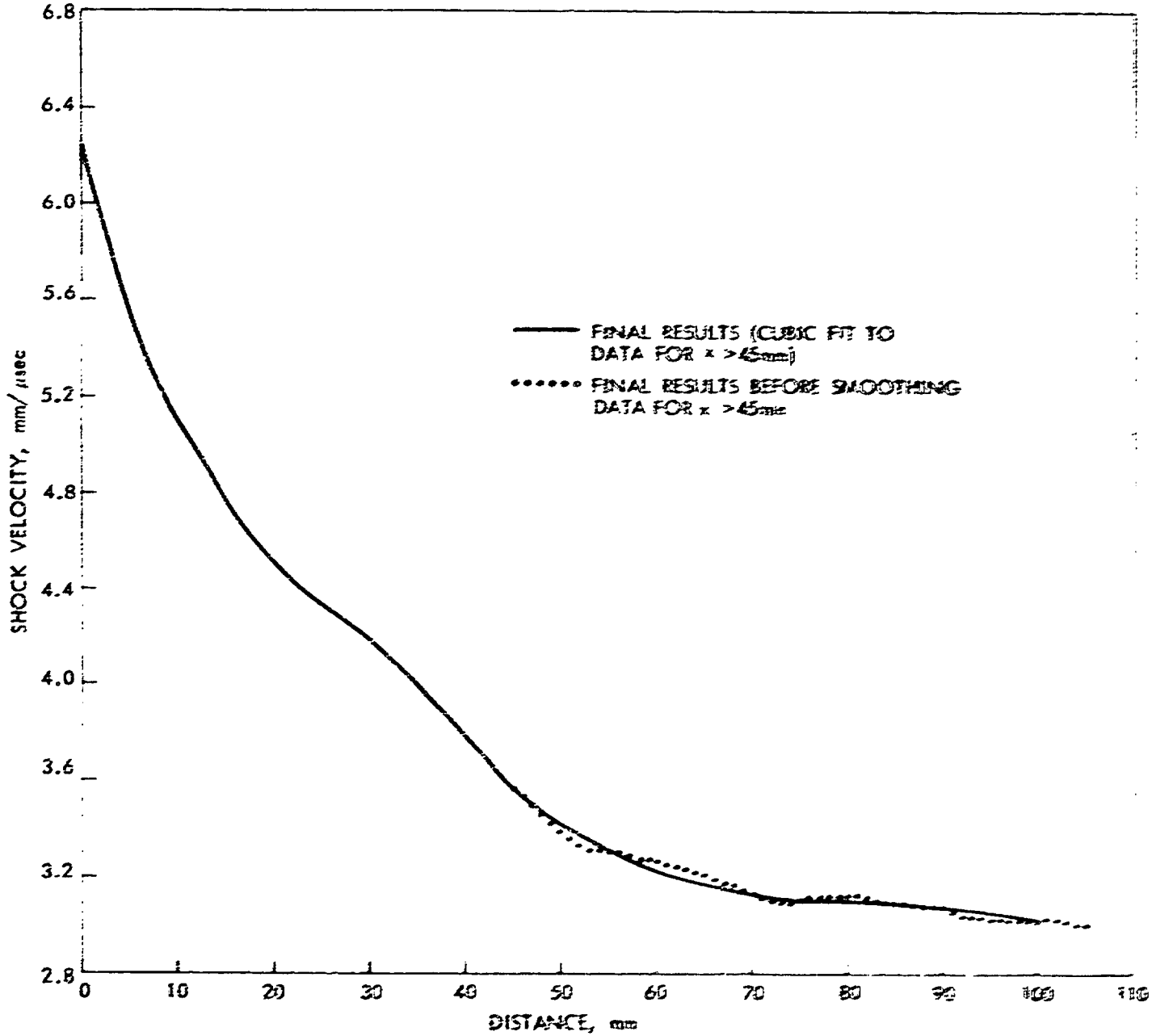


FIG. 4 SHOCK VELOCITY VS DISTANCE FOR THE LSGT WITH PENTOLITE LOADING

Table 7

COMPARISON OF SHOCK VELOCITIES FROM THREE SETS OF SHOTS USING PENTOLITE DONOR AND ONE SET USING TETRYL DONORS

| Distance mm | Shock Velocity mm/μsec | | | | |
|---|---|---|---|---|---|
| | This Work (Lot 3) | Shots 715 And 716 (Lot 2) | Shots 578 Through 580 (Lot 2) | Tetryl Calibration[1] | Pentolite Calibration[1] |
| 0.0 | 6.24 | 6.35 | 5.95 | (6.00) | (6.24) |
| 5.0 | 5.55 | 5.41 | 5.34 | (5.39) | (5.58) |
| 10.0 | 5.10 | 5.05 | 4.93 | 4.94 | 5.09 |
| 15.0 | 4.77 | 4.78 | 4.68 | 4.63 | 4.76 |
| 20.0 | 4.50 | 4.57 | 4.43 | 4.39 | 4.46 |
| 25.0 | 4.34 | 4.35 | 4.25 | 4.19 | 4.22 |
| 30.0 | 4.19 | 4.18 | 4.11 | 4.01 | 4.04 |
| 35.0 | 3.99 | 3.96 | 3.90 | 3.84 | 3.84 |
| 40.0 | 3.77 | 3.77 | 3.71 | 3.66 | 3.66 |
| 45.0 | 3.58 | 3.58 | 3.58 | 3.50 | 3.50 |
| 50.0 | 3.43 | 3.40 | 3.42 | 3.40 | 3.40 |
| 55.0 | 3.32 | 3.28 | 3.30 | 3.34 | 3.34 |
| 60.0 | 3.23 | 3.23 | 3.27 | 3.28 | 3.28 |
| 65.0 | 3.17 | 3.22 | 3.26 | | |
| 70.0 | 3.14 | 3.15 | 3.25 | 3.20 | 3.20 |
| 75.0 | 3.11 | 3.13 | 3.21 | | |
| 80.0 | 3.10 | 3.11 | 3.16 | 3.15 | 3.15 |
| 85.0 | 3.09 | 3.13 | 3.16 | | |
| 90.0 | 3.08 | 3.12 | 3.15 | 3.12 | 3.12 |
| 95.0 | 3.06 | 3.02 | 3.14 | | |
| 100.0 | 3.02 | 2.98 | 3.06 | 3.10 | 3.10 |

NOTE: Second column is for our new stock of pentolite.

Third and fourth columns are for pentolite described in reference (1).

Shot 715 - record covered $0 \leq x \leq 55$ mm
Shot 716 - covered $\sim 45 \leq x \leq 105$ mm
Shots 578 through 580 - records covered $0 \leq x \leq 110$ mm

Comparison With Previous Results. At this point it is of interest to compare the results from the preceding section with some of those obtained previously. The new results are given in Table 7, Columns 1 and 2, as well as in Figure 4. Those results in Columns 3 through 6 will be discussed in turn in the following. The explosive used in the shots represented by the data in Columns 3 and 4 is pentolite from Lot 2, see references (1) and (6).

Column 3 in Table 7 gives the results from the "close-up" shots described in reference (6). For Shot 715, the camera viewed about 50 mm of the specimen adjacent to the explosive. For Shot 716, the camera viewed the region from about 50 to 100 mm from the explosive. Values of U in Column 3 were obtained by smoothing and differentiating the data from the records as described above. The discrepancies between values of U in Columns 2 and 3 and Columns 2 and 4 for $x \leq 10$ mm are of no consequence. The reason for this is that no attempt was made to force the results given in Columns 3 and 4 to the selected value of U at $x = 0.0$. Agreement over most of the range of x is good. Note, however, the value of U at 85 mm in Column 3 is greater than the value at 80 mm. Such "oscillations" were removed from the results in Column 2 by fitting a cubic to the data for x greater than about 44 mm. The two columns are in agreement to ±1% for almost all values of $x \geq 10$ mm. This means that the two lots of pentolite are indistinguishable.

The values of U in the fourth column of Table 7 are from Shots 578, 579 and 580. They were called "regular shots" in reference (6); for these the camera recorded a field of view somewhat greater than 100 mm. These values agree with those in Column 2 less well than do those of Column 3. Note that these regular shots give values of U which are greater than those in the preceding two columns for $x > 55$ mm. Pentolite from Lot 2 was used for the shots which yielded the data in Columns 3 and 4. If we relied on the results from the regular shots (Column 4) we would conclude that pentolite from Lot 2 was more energetic than that from Lot 3, (Column 2). It is probable that the data from the close up shots (Column 3) are the more accurate, and, as noted above, the two lots of pentolite are indistinguishable when the data are obtained and reduced in the same manner.

The numbers in Column 5 of Table 7 represent the last calibration of the LSGT with tetryl. For $x \geq 55$ mm, the shock velocities of tetryl are greater than those given for the new lot of pentolite in Column 2. Because pentolite is the more powerful explosive, the opposite is expected. Again, it is probable that the new data are the more accurate; if so, the earlier tetryl calibration curve gives values of U which are too large for $x \geq 55$ mm. This difference was one of the reasons for using the electromagnetic gage to measure particle velocities in PMMA attenuators when shocked by pentolite and by tetryl.

Comparison of Column 2 with Column 5 shows that our present values of U for pentolite are greater than those for tetryl for $x < 50$ mm. This indicates, of course, that pentolite (1.56 g/cc) is more powerful than tetryl (1.51 g/cc), and that the P vs x curve of pentolite will lie above that of tetryl. The above remarks are based on the assumption that each set of results is accurate. Because different techniques were used in obtaining the two sets of data, one set may be more accurate than the other. Again, measurements of particle velocity in the PMMA attenuator help resolve the issue.

Because particle velocities have been measured in the PMMA attenuator for both explosives, there is no point in converting the values of U obtained in this section to pressures. These data will be used in a later section to help establish a Hugoniot for PMMA, which, along with the particle velocities, will determine the pressure as a function of distance.

## 4. PARTICLE VELOCITY MEASUREMENTS

Particle velocity, u, in the PMMA attenuator is measured directly using the electromagnetic velocity (EMV) gage. The gage consists of an aluminum foil (0.0005 inch thick) as shown in Figure 5a. The gage is formed by wrapping the foil around piece A where the dimension $\ell$ is carefully measured. The part of the foil around the bottom of piece A is called the base. Pieces B and C are cemented (using chloroform) to piece A and the foil and to a PMMA cylinder whose length has been measured. This whole assembly is then placed under 2000 psi for 20 minutes to remove any air bubbles. The booster pellets and the detonator holder are then added to the assembly which is placed in a magnetic field. The assembly is oriented as shown in Figure 5a, so that the shock from the donor charge causes the base of the gage to move across lines of magnetic flux, generating an emf

$$V = H \cdot u \cdot \ell \cdot 10^{-4} \qquad (7)$$

where the units are volts, gauss, mm/μsec and mm, respectively. Note that the legs of the gage do not generate an emf. The legs of the foil are attached to a coaxial cable, see Figure 5b. The 50 ohm resistor is used to impedance match the gage to the cable; the oscilloscope end of the cable is also impedance matched through a voltage divider so that two oscilloscopes can be used.

Typical oscilloscope records are shown in Figures 6a through 6c. For the record in Figure 6a, the PMMA cylinder was 5 mm long. The rise time for this record was very short, approximately 20 nanoseconds (ns). After 350 ns, the record shows some noise. This is probably induced by breaking of the PMMA or by the explosive gases

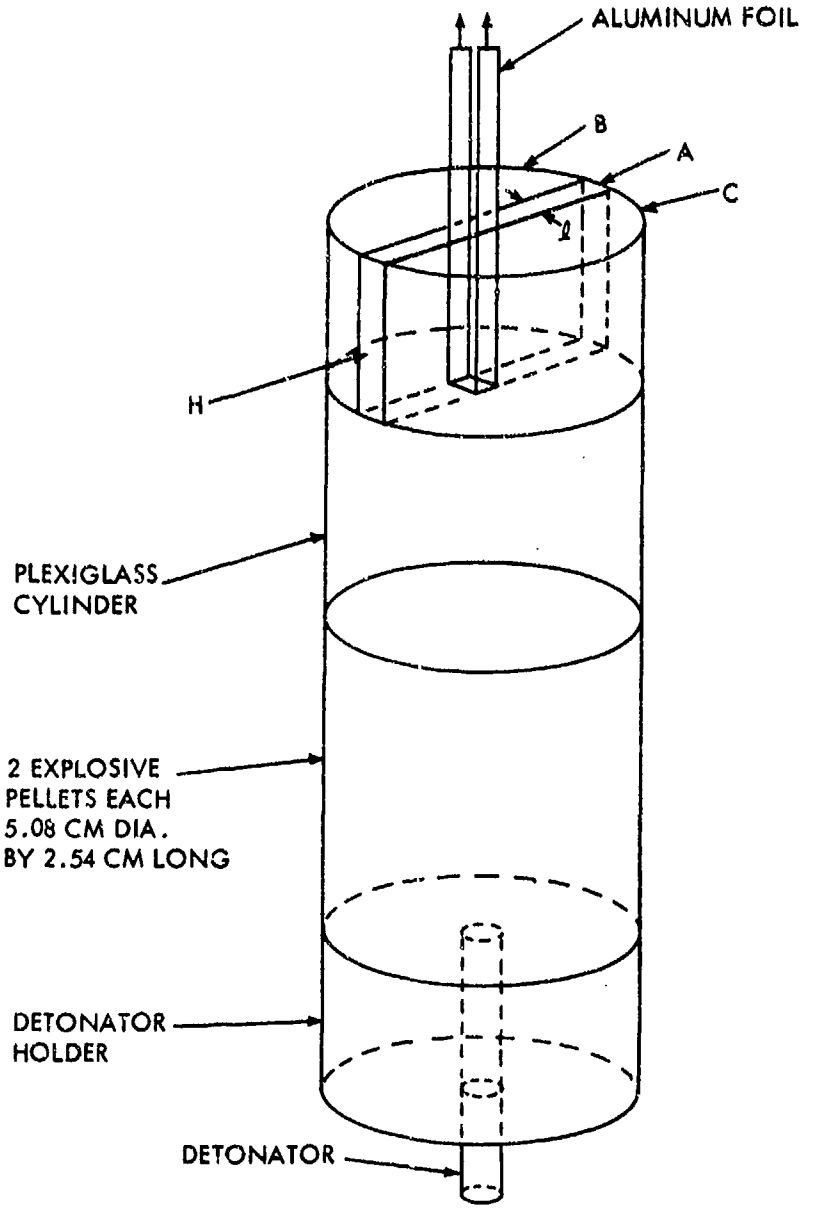


FIG. 5a EXPERIMENTAL ARRANGEMENT FOR PARTICLE VELOCITY MEASUREMENTS

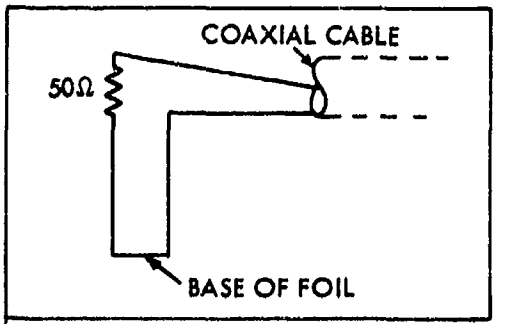


FIG. 5b ELECTRICAL CONNECTIONS TO FOIL

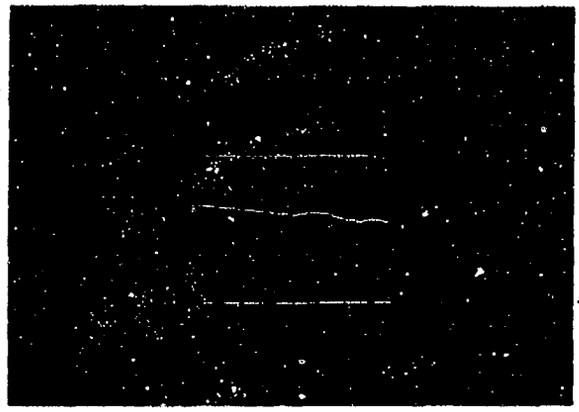

A. SHOT 258
x = 5 mm

0.39 VOLT

0.5 μ SEC

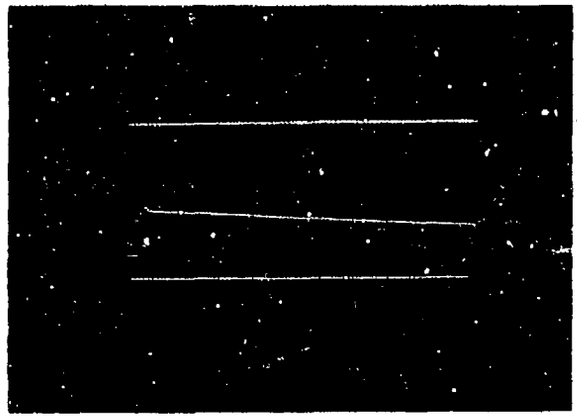

B. SHOT 230
x = 35.2 mm

0.6 VOLT

1.0 μ SEC

C. SHOT 248
x = 100.1 mm

0.11 VOLT

1.0 μ SEC

FIG. 6 TYPICAL OSCILLOSCOPE RECORDS

expanding around the edges of the PMMA cylinder. A cardboard gas shield fitted to the PMMA cylinder retards these gases sufficiently so that the noise does not destroy the usefulness of the early part of the record.

The record shown in Figure 6b is from a shot in which the PMMA cylinder was 35.2 mm long. The rise time is about 40 ns. The curious feature of the record is the overshoot which lasts about 40 ns. It is doubtful if this is a function of the circuitry. It may be due to the behavior of PMMA under rapid loading -- the material may show relaxation effects. It is possible, of course, that wave interactions actually produce such a velocity profile. The overshoot has been ignored in the determination of the peak particle velocity.

Figure 6c is a 2 microsecond record of the particle velocity for a 100.1 mm long cylinder. Rise time is again short, and there is a slight overshoot. The remainder of the record indicates that the particle velocity is relatively constant.

Records are read and digitized by using a Universal Telereader, after which plots are made; see Figure 7 for plots of the records shown in Figures 6a - 6c. The peak particle velocities can be inferred by a linear extrapolation of the curves to zero time. As noted above, the overshoot on a record is ignored. Usually, the extrapolation is based on a visually selected section of the record about 0.5 microseconds long. Most of the results were obtained by then fitting this section by least squares to a straight line over the selected interval of the record.

Peak particle velocities for tetryl donors† are given in Table 8 along with the interval of time of the record used in obtaining the peak velocity. Also included in the table are comments concerning some of the records. Asterisks following the shot number means that the record is from a Hewlett-Packard oscilloscope. The time base for these records is usually 5 microseconds so that they show less early detail than those from the Tektronix oscilloscope, for which the time base is usually 1 microsecond.

All records obtained are listed in Table 8, but some of these records were unacceptable because of noise or form (116, 121, 244, 241*) and were therefore discarded. Other records which were not used fall into two groups: (1) those obtained at $0 \leq x < 0.86$ mm and (2) those obtained with the Hewlett-Packard (HP175) oscilloscope. We found in earlier work that particle velocities above the theoretical (2.20 mm/μsec at $x = 0$ for tetryl loading of PMMA) were measured at small or no attenuation, and attributed this to the effect of the reaction zone in tetryl.[8] The reaction zone was not considered in deriving the theoretical value; instead the C-J

---

†Graphited tetryl pressed to a density of 1.51 ± 0.1 g/cc; it contains 0.5%C.

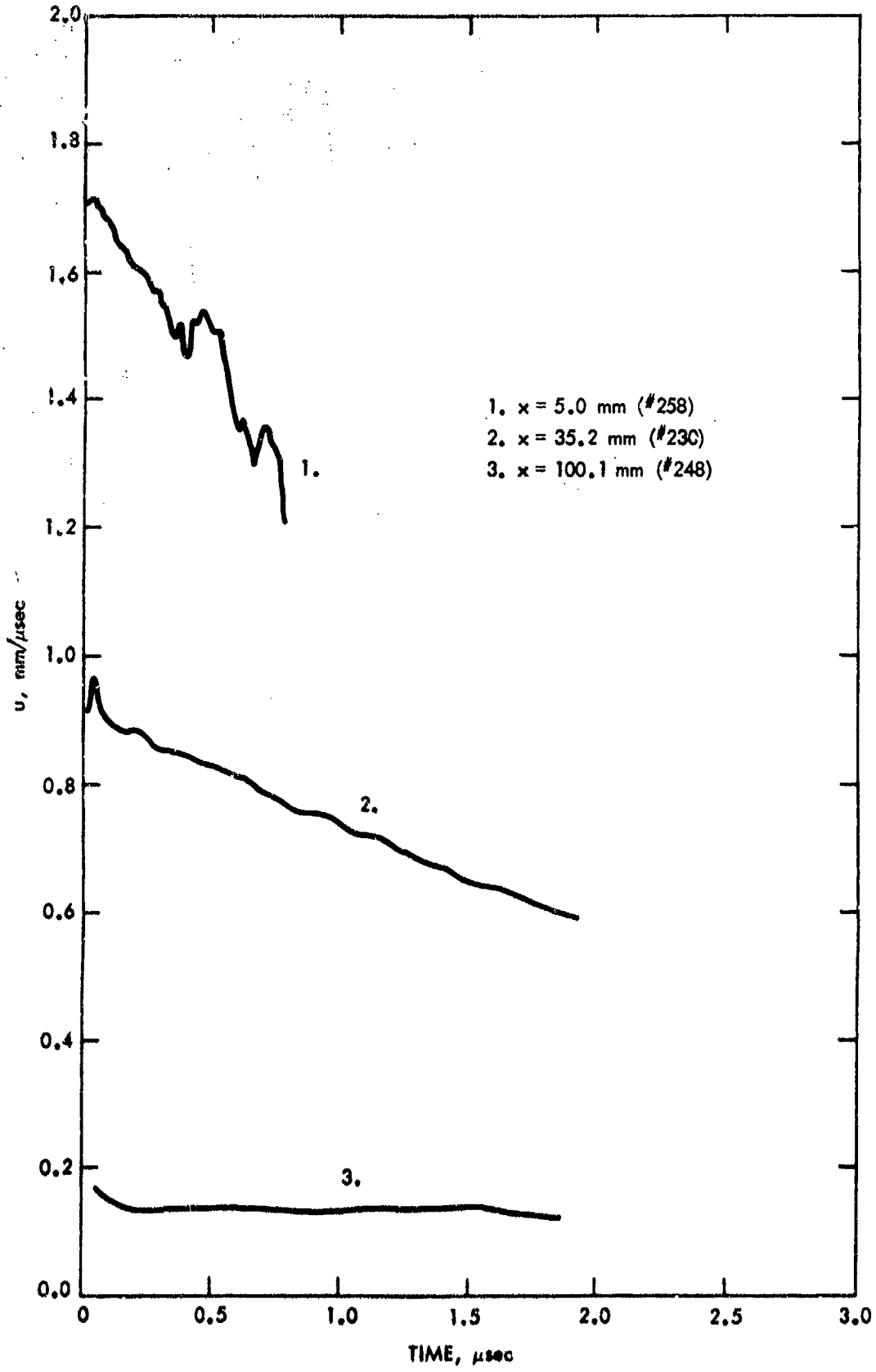


FIG. 7 PLOTS FROM RECORDS OF FIG. 6

TABLE 8

PEAK PARTICLE VELOCITIES FOR TETRYL DONOR

| SHOT NO | X MM | U MM/μSEC | TIME INTERVAL FOR LS FIT | COMMENTS |
|---|---|---|---|---|
| 289 | 0.0 | 2.11 | 0.05-0.16 | POINT INITIATED |
| 185 | 0.0 | 2.39 | | 1 MIL FOIL, PLANE WAVE BOOSTER, 25 MM OF TETRYL |
| 106 | 0.25 | 2.31 | | SOME NOISE ON RECORD, NOT USED |
| 118 | 0.25 | 2.26 | | NOT USED, RECORD ONLY 0.2 USEC LONG |
| 120 | 0.25 | 2.21 | | NOT USED |
| 108 | 0.86 | 2.25 | | |
| 183 | 0.86 | 2.22 | | |
| 119 | 2.0 | 2.05 | | |
| 117 | 3.0 | 1.88 | 0.02-0.22 | |
| 116 | 4.0 | 1.61 | 0.03-0.22 | NOISY RECORD, NOT USED |
| 241 | 5.0 | 1.74 | 0.05-0.34 | NOISY RECORD, NO GAS SHIELD |
| 244 | 5.0 | 1.78 | 0.11-0.59 | NOISY RECORD, NO GAS SHIELD |
| 241* | 5.0 | 1.76 | 0.35-1.10 | NOISY RECORD, NOT USED |
| 258 | 5.0 | 1.75 | 0.04-0.34 | GAS SHIELD REDUCED NOISE |
| 242 | 10.0 | 1.49 | 0.15-0.64 | NOISY RECORD |
| 240 | 15.0 | 1.30 | 0.16-0.33 | 0.2 USEC RISE TIME |
| 240* | 15.0 | 1.38 | 0.40-1.50 | NOT USED, COULD ALSO BE READ AS 1.30 ON PLATEAU |
| 121 | 20.0 | 1.14 | 0.02-0.20 | SHORT RECORD, FLAT, NOT USED |
| 243 | 20.0 | 1.19 | 0.13-0.64 | |
| 239* | 25.0 | 1.11 | 0.05-0.46 | OVERSHOOT |
| 231 | 30.0 | 1.01 | 0.06-0.56 | OVERSHOOT |
| 231* | 30.0 | 1.03 | 0.30-1.00 | OVERSHOOT, NOT USED |
| 222 | 35.0 | 0.892 | 0.22-0.72 | |
| 222* | 35.0 | 0.912 | 0.20-0.80 | NOT USED |
| 230 | 35.2 | 0.904 | 0.08-0.60 | OVERSHOOT |
| 230* | 35.2 | 0.91 | 0.08-0.90 | OVERSHOOT, NOT USED |
| 232 | 39.9 | 0.735 | 0.05-0.55 | |
| 232* | 39.9 | 0.741 | 0.05-0.90 | NOT USED |
| 218 | 45.0 | 0.625 | 0.10-0.60 | |
| 220 | 55.0 | 0.436 | 0.15-0.65 | OVERSHOOT |
| 220* | 55.0 | 0.44 | 0.14-0.90 | NOT USED |
| 233 | 65.1 | 0.309 | 0.06-0.65 | |
| 234 | 80.1 | 0.192 | 0.06-0.56 | |
| 246 | 80.0 | 0.20 | 0.15-0.63 | OVERSHOOT |
| 245 | 89.6 | 0.126 | 0.10-0.98 | NOT USED |
| 247 | 89.8 | 0.169 | 0.14-0.66 | |
| 223 | 100.0 | 0.151 | 0.29-1.00 | OVERSHOOT |
| 248 | 100.1 | 0.135 | 0.11-0.64 | OVERSHOOT |

*HEWLETT-PACKARD 175 OSCILLOSCOPE, TIME BASE CA. 5 μSEC. ALL OTHER RECORDS FROM TEKTRONIX 454 OSCILLOSCOPE, TIME BASE CA. 1 μSEC

pressure at the end of the reaction zone was used as the loading pressure of the PMMA. Subsequent work has shown that measurements at small attenuation are not reproducible; this is attributed to the very steep slope of the pressure-time curve produced by the standard tetryl donor of the LSGT. For this reason, all values at $x < 10$ mm are considered nominal even in the range $x \geq 0.86$ mm where measurements of u seem reproducible. Moreover, this nominal range is started ($x = 0$) at a value measured with a plane wave boosted tetryl loading of the PMMA. Beyond $x \geq 10$ mm, the original pressure spike has been broadened so that its duration seems sufficient to impart a particle velocity to the foil consistent with the maximum amplitude of the pressure pulse. In group (1), Shots 289, 106, 118, and 120 have not been used.

In group (2), the HP175 records are, with one exception, from the same shots on which Tektronix records were made. Since we consider the latter to be in principle more accurate, the only HP record we have used is that from Shot 239 on which no Tektronix record was obtained. The justification for using that particular record is the generally close agreement between the HP and Tektronix results for the same shot, as shown by the data of Table 8.

The data selected, as above, from Table 8 are plotted in Figure 8a which also shows two additional points rejected for inconsistency with the rest of the data. The final calibration data have been joined by use of a French curve. That was done as a preliminary to further study, and to illustrate the marked similarity between the u-x curve of Figure 8a and the U-x curve of Figure 4 (previous section) in exhibiting "humps" centered at x = 30-35 mm.

It is important to note that the data retained at $x = 0$ is from Shot 185; this used a 0.001 inch thick foil, a plane wave booster and only 25 mm of tetryl. This configuration gives a larger velocity (by 0.28 mm/μsec) than that using 51 mm of tetryl initiated at a point; see Shot 289 in Table 8. The reason for this is that the plane wave configuration gives a longer pulse to which the foil can respond more readily. Thus the results are more representative of the particle velocity at the interface than are those from point detonated charges.

An estimate of the precision of the measurements shown in Figure 8a can be obtained by examining the replicate (or nearly so) shots listed in Table 9. The absolute differences within the sets varies from 0.008 to 0.04 mm/μsec. These ranges, as percentages of the average value of the set of replicate shots, vary from 0.9 to 11.2%. (The value of 32% at $x \approx 90$ mm has been rejected as intolerable, and the data of Shot 245 have been discarded as inconsistent with values observed at the adjacent stations, $x = 80$ and $x = 100$ mm. See Figure 8a.) Because the measured value u varies by a factor of 10 for $5 \leq x \leq 100$ mm, it is not possible to obtain the same percentage error over the range. At 5 mm, the shock is attenuating rapidly and the flow of the detonation products frequently causes

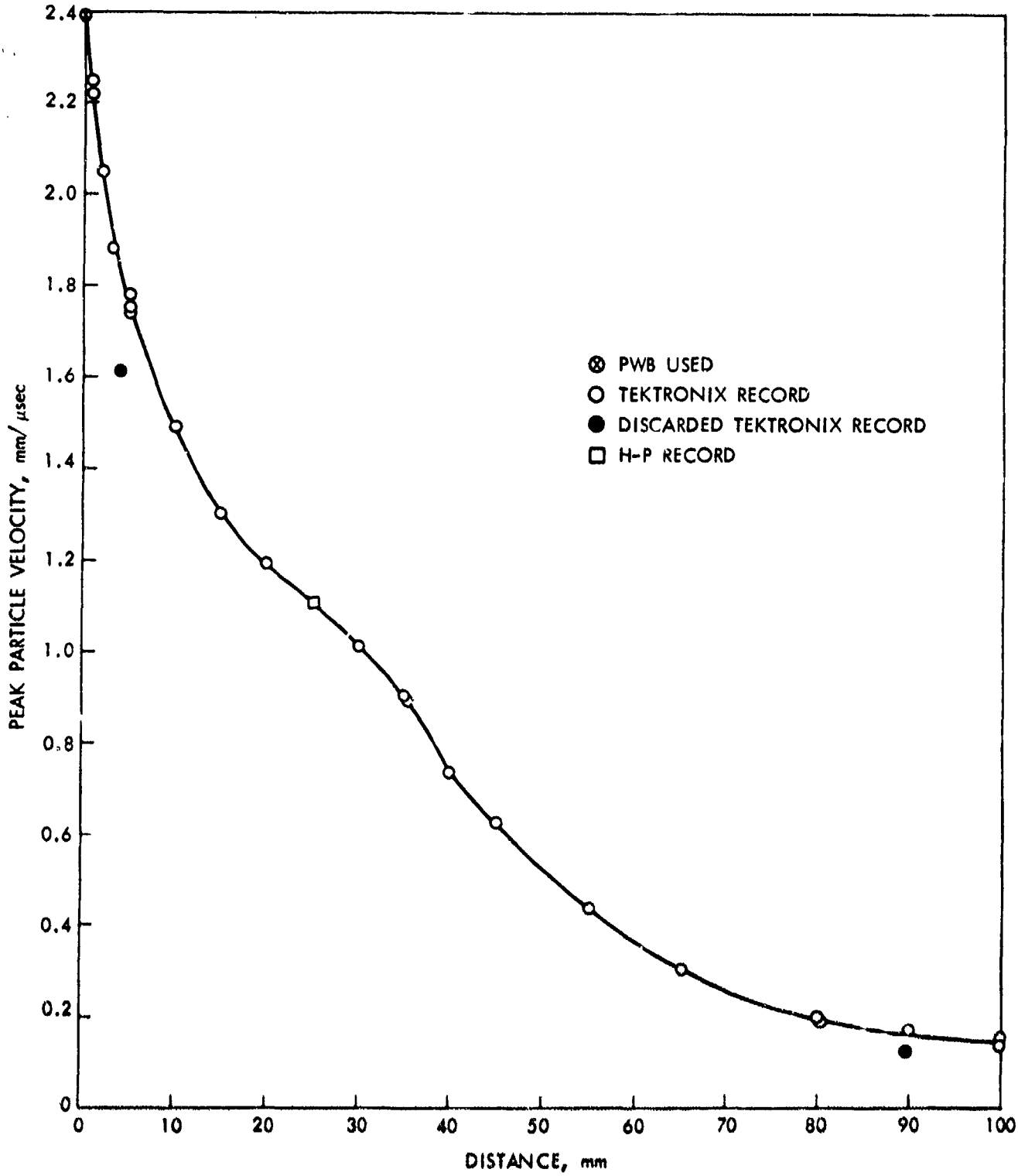


FIG. 8a EXPERIMENTAL RESULTS, TETRYL DONOR

Table 9

RESULTS FROM REPLICATE SHOTS (TETRYL DONOR)

| Shot # | x mm | Peak Particle Velocity mm/μsec | Range mm/μsec | 100 x range, % average |
|---|---|---|---|---|
| 241 | 5.0 | 1.74 | | |
| 244 | 5.0 | 1.78 | 0.040 | 2.3 |
| 258 | 5.0 | 1.75 | | |
| 222 | 35.0 | 0.912 | | |
| 230 | 35.2 | 0.904 | 0.008 | 0.9 |
| 234 | 80.1 | 0.192 | | |
| 246 | 80.0 | 0.200 | 0.008 | 4.1 |
| 245 | 89.6 | 0.126* | | |
| 247 | 89.8 | 0.169 | 0.043 | 32.0* |
| 223 | 100.0 | 0.151 | | |
| 248 | 100.1 | 0.135 | 0.016 | 11.2 |

*Rejected on basis of consistency.

electrical noise. Here, the value of u is relatively large, so that a range of 0.04 in the value of u does not make a large percentage error. At 100 mm, the shock is attenuating very little, and the difference between values, 0.016 is small. As a percentage, however, the range is large because of the small magnitude of u. At this time, we cannot measure values of u as small as 0.15 mm/μsec as precisely as we would like to.

Another approach to estimating the error in an EMV gage measurement is given in the Appendix. That estimate is for the determination of a single value of u from an oscilloscope record. The results are useful here, even though we have been discussing peak values of u which we obtain by fitting the data to a straight line and extrapolating back to zero time. The estimated error ranges from 6.2% for u = 0.10 mm/μsec to 5.6% for u = 2.0 mm/μsec. The slight variation of the error with the magnitude of u is due to the reading of the calibrating voltage on a three digit voltmeter. With a more precise voltmeter, the error would be independent of the value of u. This comes about because we change the gain of the oscilloscope amplifier so that we have about the same deflection on the record regardless of the actual value of u which is expected. This is equivalent to changing scales, for example, on a voltmeter, so that all readings are taken with about the same deflection of the indicator. This independence of the estimated error of the magnitude of the value of u is counter to our experience with replicate shots as described above. This disagreement may be due to the fact that our experimental arrangements are not reproducible, as noted in the Appendix.

Figure 8b shows the calibration data and the data computed using WONDY[9] for tetryl loading of PMMA. Although the two curves seem nearly the same at small x values, the experimental is definitely above the computed curve in the range $15 \leq x \leq 35$ mm. Possible reasons for this are one or more of the following:

a. Our extrapolation procedure leads to too high values of u.

b. The shock loading pressure (C-J, not von Neumann) from tetryl was too low.*

c. The Hugoniot used for PMMA was inaccurate.

Case a alone is quite inadequate to explain the discrepancy. The velocity of the gage should be equal to or less than the material velocity. Hence if we replace the values obtained by extrapolating to zero time with the maximum value of u actually recorded, it should be ≤ the true particle velocity. Examination of the records shows that

---

*Because of zoning in the tetryl, the actual value of the pressure in the computation will be less than the nominal C-J pressure which it approaches only as the zone size approaches zero. In the WONDY computation the zone size was 0.05 cm in tetryl and 0.01 cm in PMMA.

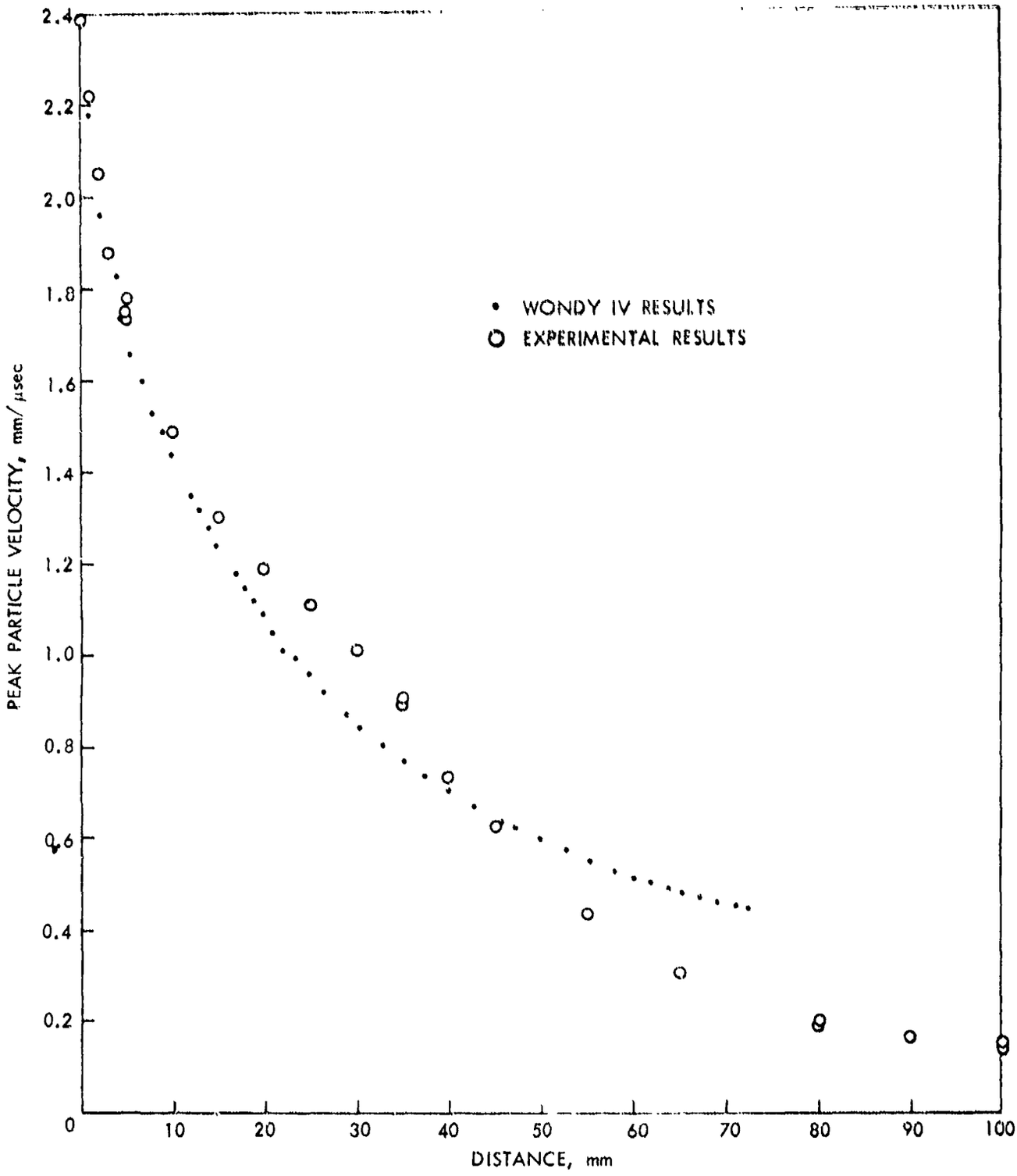


FIG. 8b EXPERIMENTAL RESULTS COMPARED WITH RESULTS COMPUTED USING WONDY

such a procedure in this range of x lowers the u value by 0.03 mm/μsec at most; the difference we wish to explain is about 5x this value.

We have already mentioned that C-J conditions were used in the computations instead of von Neumann conditions. Hence the leading shock pressure used (case b) was too low, or too much lowered by the zone size, or both. The Hugoniot data used (case a) was that derived from the previous LASL calibration, and hence less accurate than those derived from the present work. Case b, too low an initial pressure, seems the likeliest single cause for the unexpected relation, u (experimental) > u (computed).

We make the assumptions that the Hugoniot used will give a u-x curve of approximately the correct shape, and that the shock loading pressure, as used in the computations, was too low. Accordingly, the WONDY curve of Figure 8b has been raised (by 0.125 mm/μsec) in Figure 8c so that it approximates the experimental curve in the range $0 \leq x \leq 35$ mm. This illustration strongly suggests that the on-axis flow is one-dimensional for $0 \leq x \leq 35$ mm, and becomes two-dimensional with the arrival of strong lateral rarefaction waves at about $x = 35$ mm. This suggestion is reinforced by the data treatment which will now be described.

Figure 8a could be used to make graphical interpolations between data points. However, analytical relations which fit the data are far more convenient for interpolation. Moreover, in this case such fits prove helpful in interpreting the data.

A polynomial could be used to fit the data over the entire range of x, or a set of polynomials could be used to fit subsets of the data. (In this case, a curve very like the U-x curve of Figure 4 of the previous section would probably be obtained). Polynomials have bad features, as has been related before.[7] In an attempt to discover a more appropriate function, the data were plotted on semi-log paper. On the semi-log plot shown in Figure 9, the data between 0 and 35 mm appear to be exponential in a manner similar to that found in the radioactive decay of two isotopes having significantly different half-lives. The appropriate function seems to be:

$$u = A \exp(-Bx) + C \exp(-Dx) \qquad (8)$$

This function fits the data very well; see Table 10. The coefficients, in the order in which they appear in the above equation, and their quadratic mean errors (QME's) are:

| Coefficient | QME |
|---|---|
| 1.7342 | 0.043 |
| 0.01852 | 0.001 |
| 0.6602 | 0.041 |
| 0.2794 | 0.030 |

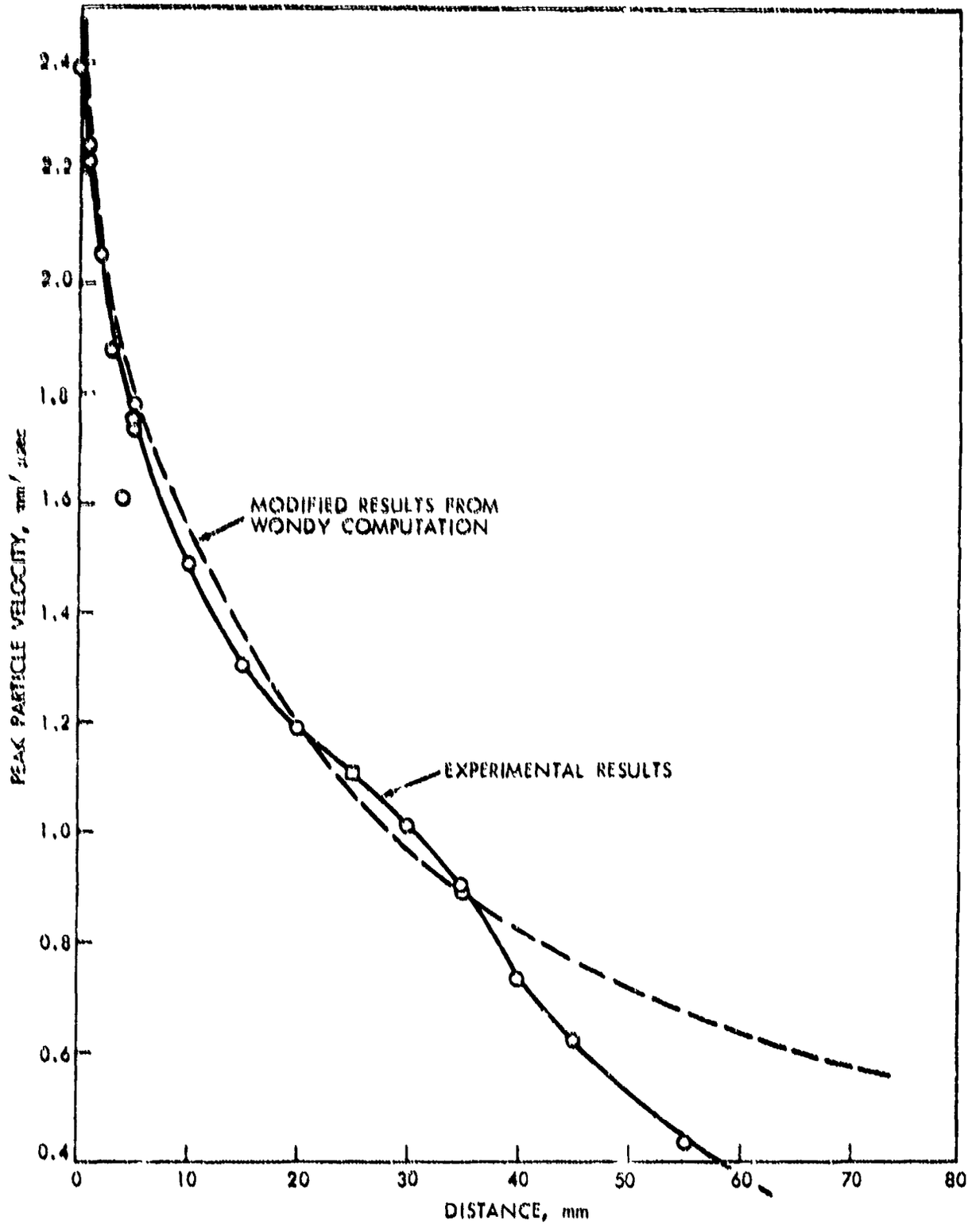


FIG. 8c EXPERIMENTAL RESULTS COMPARED WITH MODIFIED RESULTS COMPUTED USING WONDY

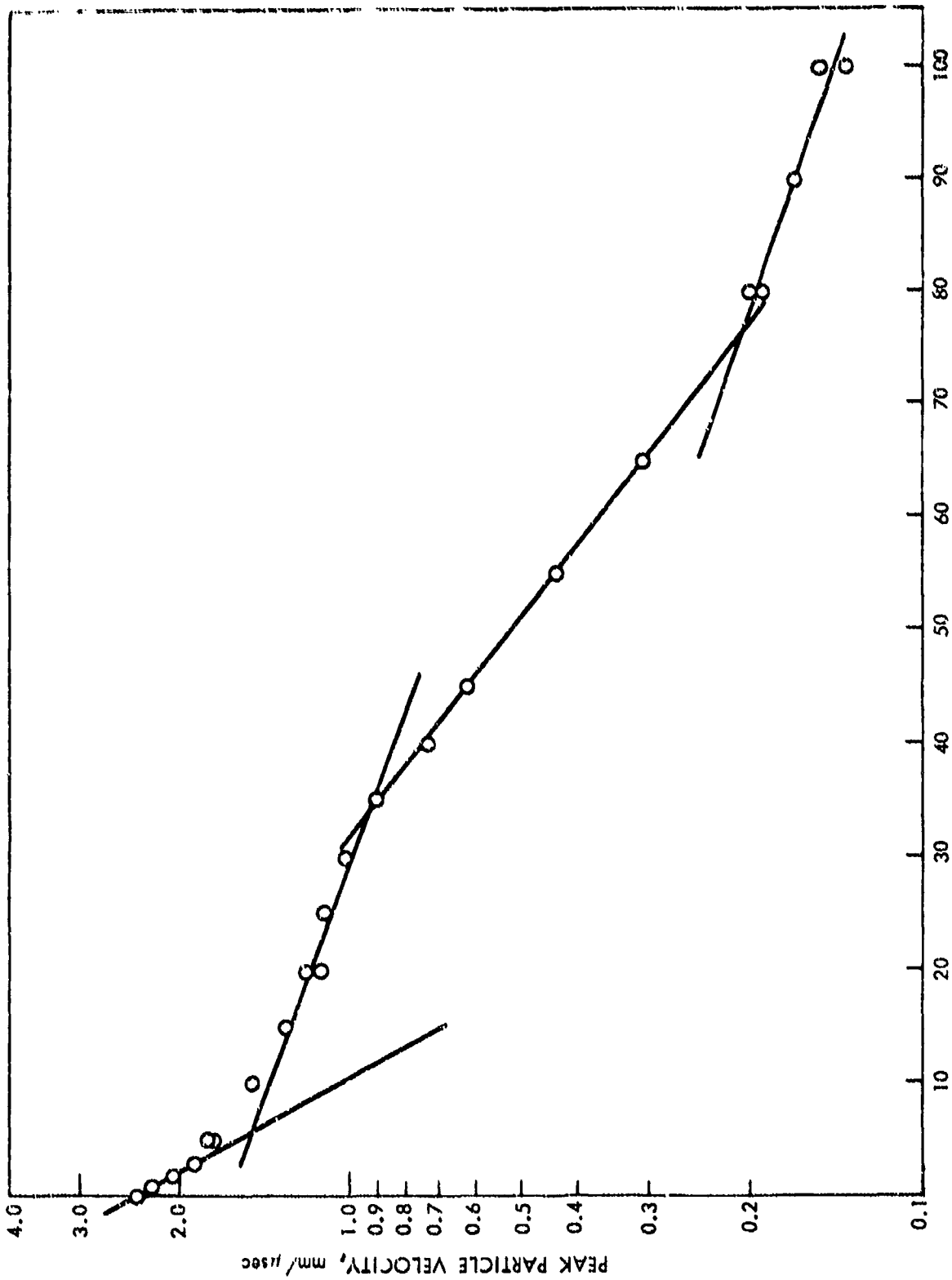


FIG. 9 SEMILOG PLOT OF EXPERIMENTAL DATA (TETRYL DONOR)

Table 10

FIT TO TETRYL D [illegible] FOR $x \leq 35.2$ mm
FUNCTION IS $u = A \exp(-Bx) + C \exp(-Dx)$

| x mm | u mm/μsec | u (Calculated) mm/μsec | Residuals mm/μsec |
|---|---|---|---|
| 0.00 | 2.390 | 2.39441 | .004 |
| 0.86 | 2.250 | 2.22600 | -.024 |
| 0.86 | 2.220 | 2.22600 | .006 |
| 2.00 | 2.050 | 2.04874 | -.001 |
| 3.00 | 1.880 | 1.92604 | .046 |
| 5.00 | 1.740 | 1.74415 | .004 |
| 5.00 | 1.780 | 1.74415 | -.036 |
| 5.00 | 1.750 | 1.74415 | -.006 |
| 10.00 | 1.490 | 1.48141 | -.009 |
| 15.00 | 1.300 | 1.32354 | -.024 |
| 20.00 | 1.190 | 1.19983 | -.010 |
| 25.00 | 1.110 | 1.09206 | -.018 |
| 30.00 | 1.010 | 0.99506 | -.015 |
| 35.00 | 0.892 | 0.90694 | .015 |
| 35.20 | 0.904 | 0.90358 | .000 |

The QME of the fit is 0.019. The residuals are given in the fourth column of Table 10. The largest residual is for x = 3.0 mm; it is 0.046, or about 2.5% of the measured value. A residual of this size is tolerable in view of the range between replicates as discussed above, and also that x = 3 mm is within the range of "nominal" calibration. Outside this range of u, (i.e., x < 10 mm) the largest residual, on a percentage basis, is 1.8%.

There appears to be a distinct change in the slope of the u vs x relation at about 35 mm, see Figure 8c. Data beyond 35 mm must be fitted with another function. As shown in the semi-log plot of Figure 9, two straight lines can be drawn through the data; the first serves for $35 \leq x \leq 75$ mm, while the second serves for $75 \leq x \leq 100$. Thus it appears, at first glance, that two or more functions are required, and that a distinct change in slope might be introduced at 75 mm. An examination of Figure 8a shows that a discontinuity in the slope of the u-x curve at 75 mm is not evident. Moreover, it is not necessary to separate these data into two subsets for x > 35 mm. The strategy is to fit the quantity (u - A) vs x. That is, subtracting a judiciously chosen value of A from the values of u yields a straight line plot on semi-log paper. The results of such a fit are given in Table 11. The coefficients and their QME's for the relation

$$u = A + B \exp(-Cx) \tag{9}$$

are

| Coefficient | QME |
|---|---|
| 0.0921 | 0.0065 |
| 3.7038 | 0.135 |
| 0.0435 | 0.0011 |

The QME of the fit, 0.008, is about half of the QME of the fit given in Table 10. Examination of the residuals shows that the fit is really very good, considering that the function has only 3 parameters. Unavoidably, the residuals for very low u values are a high percentage of u.

It must be noted in passing that some of the data shown in Table 11 are from shots using pentolite donors. In a later section, it will be noted that tetryl and pentolite give values of particle velocity which are not distinguishable at high attenuations. Hence, the u vs x curves are allowed to converge for some value of x less than 80 mm.

Note that in Table 11, two or three values of u are given for several individual values of x. If all values of u were given the same weight, the function would have fitted these multivalued points more closely than the single value points. This was prevented by giving the multivalued points a weight of 1.0, while the single valued points were given a weight of 2.0.

Table 11

FIT TO TETRYL DATA FOR $x \geq 35$ mm
AND PENTOLITE DATA FOR $x \geq 80$ mm
THE FUNCTION IS $u = A+B \exp(-Cx)$

| x mm | u mm/μsec | Weight | u (Calculated) mm/μsec | Residual mm/μsec |
|---|---|---|---|---|
| 35.0 | .89200 | 1.0 | .90010 | .008 |
| 35.2 | .90400 | 1.0 | .89310 | -.011 |
| 39.9 | .73500 | 2.0 | .74499 | .010 |
| 45.0 | .62500 | 2.0 | .61509 | -.010 |
| 55.0 | .43600 | 2.0 | .43061 | -.005 |
| 65.1 | .30900 | 2.0 | .31025 | .001 |
| 80.0 | .20000 | 1.0 | .20620 | .006 |
| 80.0 | .19400 | 1.0 | .20620 | .012 |
| 80.1 | .19200 | 1.0 | .20571 | .014 |
| 89.8 | .16900 | 1.0 | .16660 | -.002 |
| 100.0 | .15100 | 1.0 | .13991 | -.011 |
| 100.0 | .14100 | 1.0 | .13991 | -.001 |
| 100.1 | .13500 | 1.0 | .13970 | .005 |
| 101.6 | .14800 | 1.0 | .13670 | -.011 |

Figure 10 shows the u-x data plotted along with the solid lines of the fitted equations (Equations (8) and (9)). This treatment has resolved the "hump" of Figure 8a into a cusp between the two analytic curves near x = 35 mm, at about the location of the maximum amplitude of the so-called hump. Figure 10 illustrates much more clearly than Figure 8c, the termination of one-dimensional flow by the arrival of a lateral rarefaction at the axis.

Not enough measurements were made in the earlier work to reveal the cusp which is evident in the new data at about 35 mm. It appears that the slope of the u vs x curve changes abruptly at this distance. This is doubtlessly caused by the interaction of rarefaction waves which originate at the periphery of the PMMA cylinder at the interface between it and the explosive. The strength of this rarefaction increases because of radial convergence. When it reaches the axis of the PMMA cylinder, it causes an abrupt change in the flow due not only to its strength but also to the gradient of flow variables across it. Another manifestation of this wave interaction was pointed out in a previous section where the shock velocity was measured as a function of x. Indeed, the similarities of Figures 4 (previous section) and 8a indicate that a similar analytical treatment of the U-x data might result in showing a cusp at x = 35 mm in the shock velocity data also.

Kamegai and Erkman[10] used a two-dimensional elastic-plastic code, HEMP, to study the diverging shock wave in the PMMA in the LSGT configuration. This earlier work was done without knowledge of the particle velocity measurements discussed above. Two different grid sizes, 0.06 cm sq. and 0.12 cm sq., were used in the 2-D work. Unfortunately, only the 0.12 cm sq. zone results covers the range 0 to 100 mm. As shown in Figure 11, the 2-D study reproduces the shape of the u vs x curve obtained by the EMV method but the code results are larger. These larger values of u may be due to the use of a smaller value of $\gamma$ (and correspondingly higher value of $P_{CJ}$) for the explosive gases; a $\gamma$ of 2.54 was used while experimental work[11] yields a $\gamma$ of 3.00. With this in mind, the calculated and experimental u vs x curves agree well. Shifting the computed curve down about 0.07 mm/μsec gives better agreement, of course, and, more important, clearly illustrates the same type of abrupt change in slope at ≈ 35 mm in the computed curve. An analytical treatment similar to that used on the experimental data might well demonstrate a cusp in the 2-D curve,* and appears to be a more reliable way to locate the arrival of the lateral rarefaction than the method chosen in reference (10). That method was based on finding where the calculated shock front deviated from spherical expansion. The result was that the flow seemed to be spherical out to ≈ 50 mm where the side rarefaction finally reached the axis of the cylinder. It now

---

*Of course, 2-D computations of more closely spaced points should do the same thing.

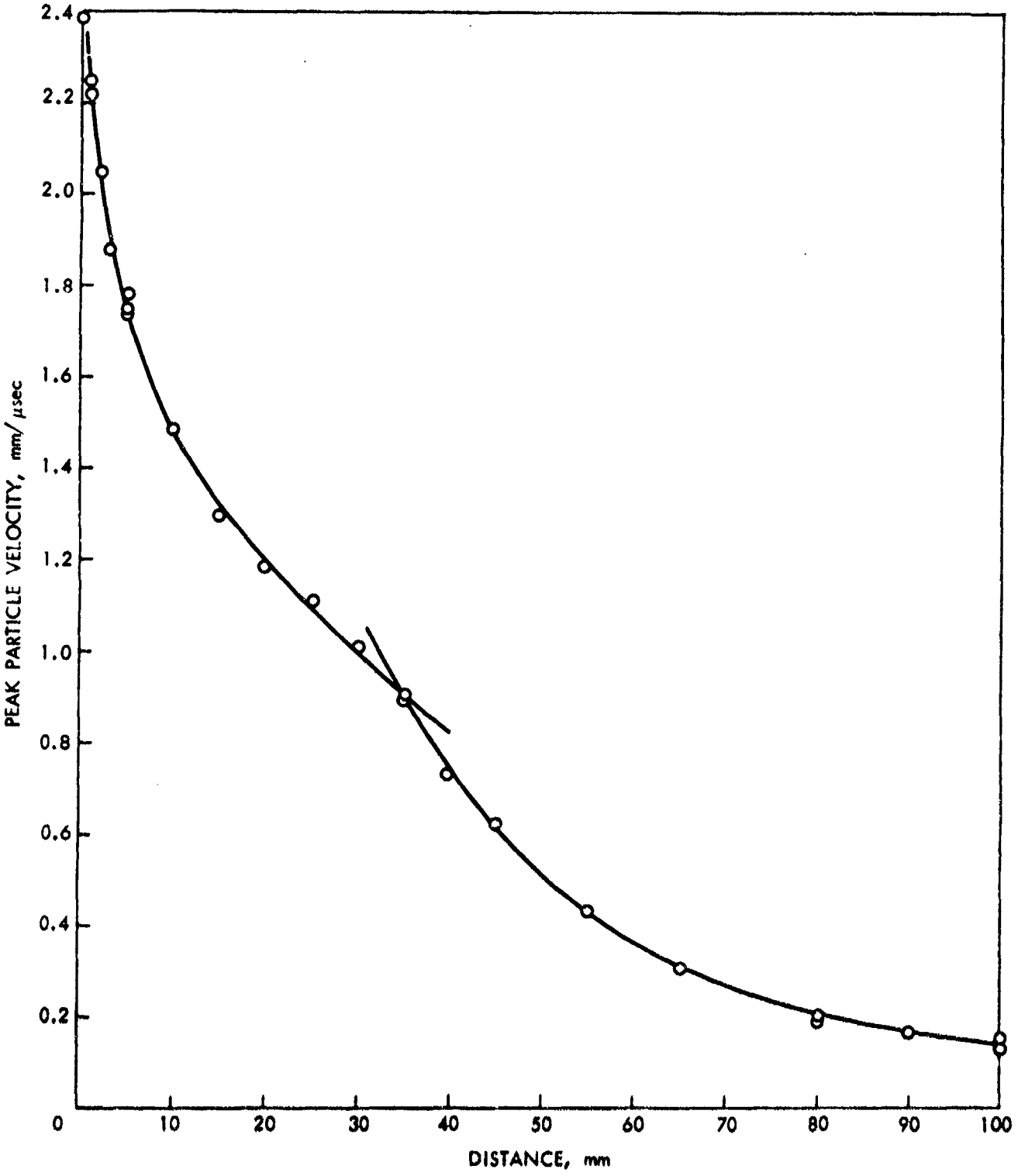


FIG. 10 RESULTS OF FITTING PEAK PARTICLE VELOCITIES VS DISTANCE (TETRYL DONOR)

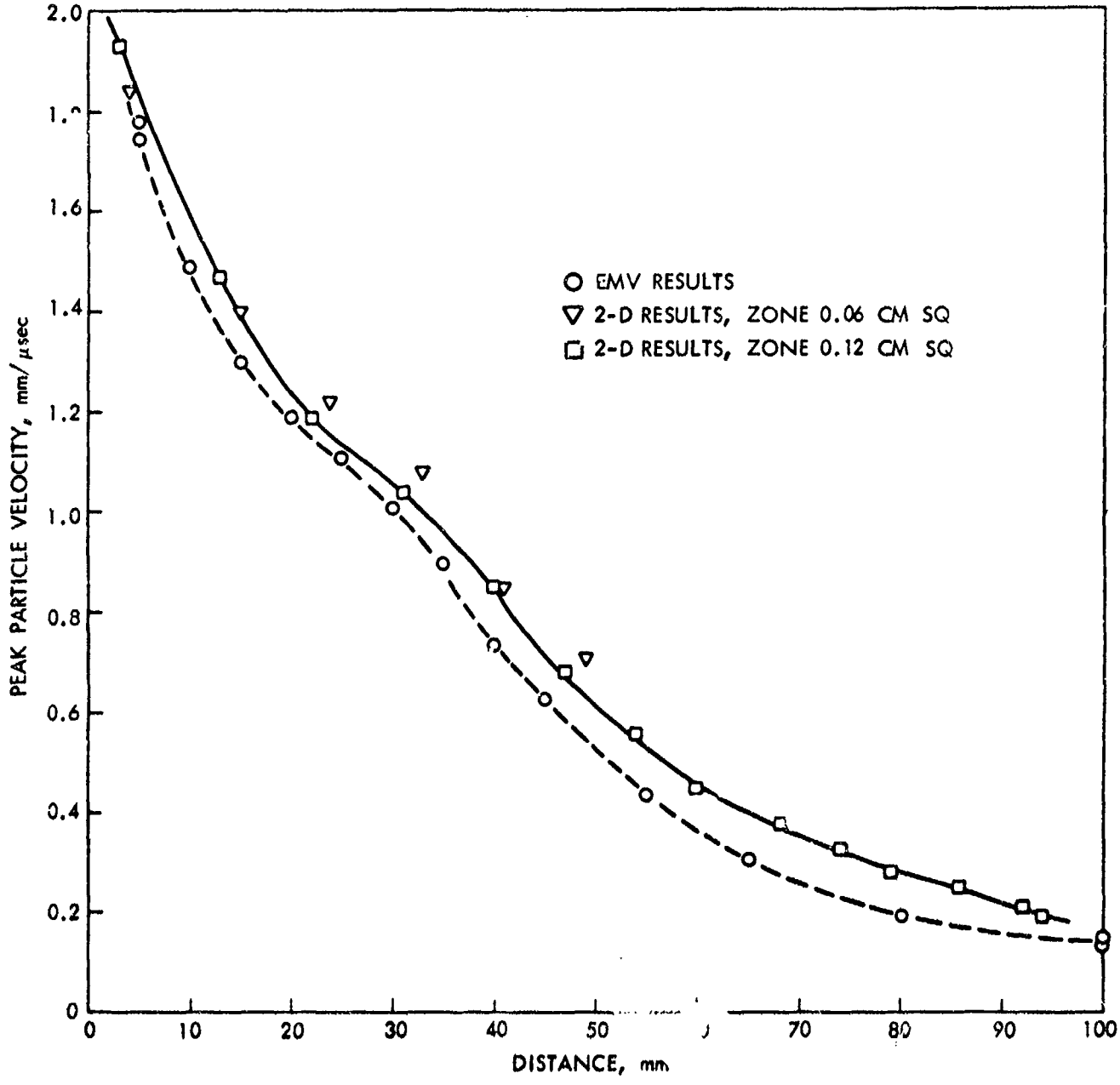


FIG. 11 COMPARISON OF EXPERIMENTAL RESULTS WITH RESULTS COMPUTED USING THE HEMP CODE

appears that the front is affected by lateral rarefactions at about 35 mm; beyond that distance the shock is two-dimensional.

In previous work, velocities of the free surfaces of the ends of cylinders such as shown in Figure 5a were measured. If the shocked PMMA behaves as an inviscid fluid, the particle velocity is half the measured free surface velocity. Figure 12 shows the difference between this estimate and the measured particle velocities in PMMA. Representative values are as follows:

| Gap Length mm | u, mm/μsec | | Difference mm/μsec |
|---|---|---|---|
| | Free Surface Method | EMV Method | |
| 20 | 1.09 | 1.19 | 0.10 |
| 45 | 0.54 | 0.63 | 0.09 |
| 75 | 0.21 | 0.22 | 0.01 |
| 100 | 0.145 | 0.151 | 0.006 |

The free surface method gives significantly smaller values of u at 20 and 45 mm. At 75 and 100 mm the two methods are in substantial agreement. Thus the new work shows significantly larger particle velocities of moderate (and presumably, low) attenuations; this will result in larger pressure also. It is chiefly the improvement in values of u that requires the present recalibration of both the tetryl and the pentolite loaded PMMA.

Data from shots using pentolite donors are given in Table 12 and in Figure 13. Table 12 has the same format as Table 8 for ease in comparing results. Another aid in comparing the two sets of data is the curve in Figure 13 which represents the fits to the tetryl data. For $10 \leq x \leq 65$ mm, pentolite donors give slightly greater values of u. This is to be expected because pentolite has an estimated Chapman-Jouguet pressure of 216 kbar while tetryl has a CJ pressure of 190 kbar.[11] This difference, for some unknown reason, is not apparent in our data for $x < 10$ mm.

It should be remarked at this point that for any $x > 10$ mm, the difference between u measured for pentolite and tetryl loading is experimentally insignificant. This is indicated both by our error analysis and by the range found for replicate measurements. However, most pentolite data were consistently above the analogous tetryl data. Hence we have presented two distinct calibration (u-x) curves with the small differences between them shown in Figure 13.

Again, we report results from the Hewlitt Packard oscilloscope but do not use them in the subsequent curve fitting. Results of Shot 260 were not used because of the use of a "radial foil" (i.e., the leads from the pickup came out of the PMMA cylinder parallel to a radius rather than as shown in Figure 5a). Shot 261 was rejected because it gave results that were less than those in tetryl shocked PMMA at the same position. The same is true of Shot 210.

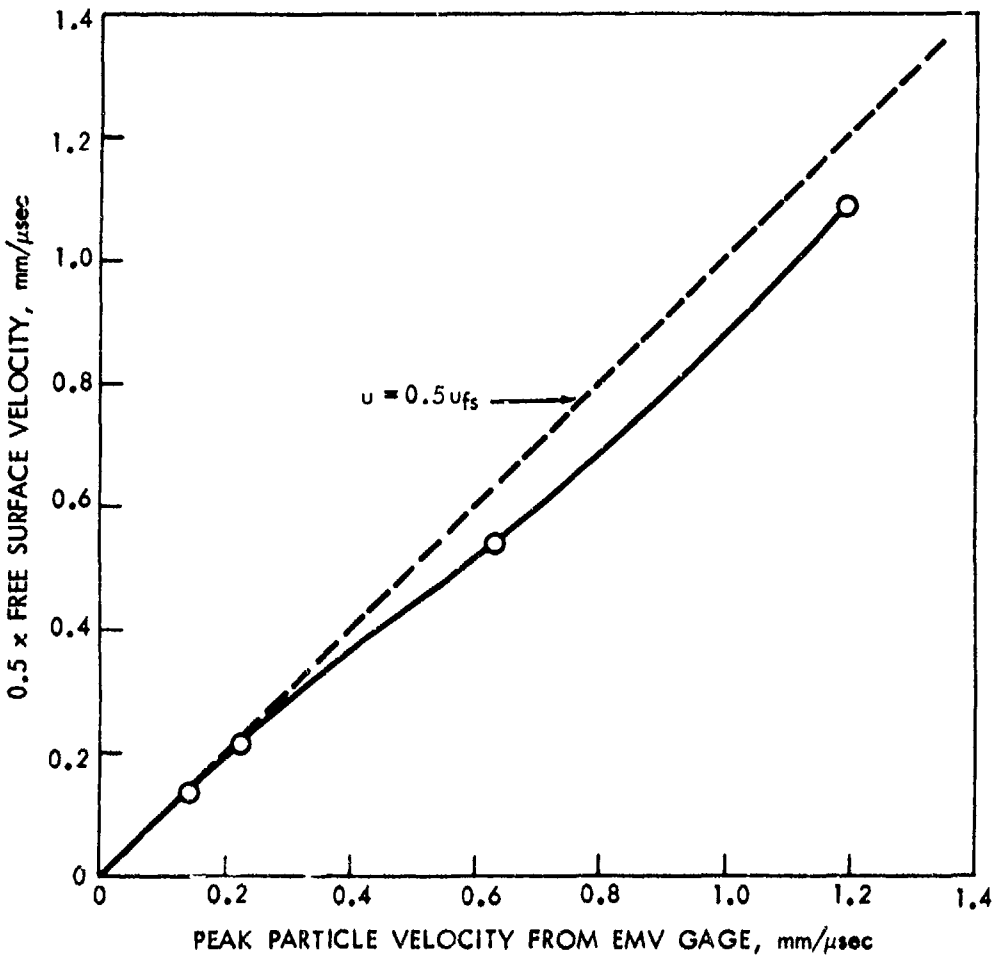


FIG. 12 DIFFERENCE BETWEEN u FROM FREE SURFACE VELOCITY MEASUREMENTS AND FROM EMV GAGE MEASUREMENTS (TETRYL DONORS)

TABLE 12

PEAK PARTICLE VELOCITIES FOR PENTOLITE DONOR

| SHOT NO. | X MM | U MM/μSEC | TIME INTERVAL FOR LS FIT | COMMENTS |
|---|---|---|---|---|
| 286 | 0.0 | 2.37 | 0.06-0.17 | |
| 277 | 5.0 | 1.80 | 0.03-0.45 | |
| 278 | 5.0 | 1.74 | 0.018-0.96 | |
| 275 | 10.0 | 1.494 | 0.05-0.54 | |
| 261 | 10.0 | 1.39 | 0.12-0.63 | NOT USED, LOWER THAN TETRYL |
| 262 | 10.0 | 1.51 | 0.09-0.35 | |
| 276 | 15.0 | 1.351 | 0.10-0.55 | |
| 263 | 20.0 | 1.257 | 0.13-0.63 | |
| 264 | 20.0 | 1.22 | 0.04-0.39 | OVERSHOOT |
| 270 | 25.0 | 1.12 | 0.13-0.65 | |
| 260 | 25.0 | 1.09 | 0.10-0.60 | RADIAL FOIL, NOT USED |
| 271 | 25.0 | 1.11 | 0.05-0.56 | TYPICAL RECORD |
| 235 | 30.0 | 1.038 | 0.06-0.45 | TYPICAL RECORD |
| 235* | 30.0 | 1.05 | 0.20-1.50 | NOT USED |
| 265 | 30.0 | 1.01 | 0.07-0.56 | |
| 225 | 35.0 | 0.942 | 0.05-0.55 | |
| 225* | 35.0 | 0.945 | 0.10-0.85 | NOT USED |
| 229 | 38.1 | 0.826 | 0.05-0.55 | TEST WITH TWO PIECES OF PMMA, NOT USED |
| 236 | 39.9 | 0.786 | 0.03-0.47 | |
| 236* | 39.9 | 0.787 | 0.20-1.00 | NOT USED |
| 219 | 45.0 | 0.661 | 0.09-0.60 | |
| 210 | 45.0 | 0.613 | 0.10-1.10 | LESS THAN TETRYL AT SAME DISTANCE |
| 211 | 54.9 | 0.431 | 0.27-1.09 | |
| 221 | 55.0 | 0.451 | 0.07-0.60 | |
| 237 | 65.1 | 0.313 | 0.03-1.00 | EYE FIT IS USED |
| 266 | 80.0 | 0.194 | 0.09-0.54 | |
| 224 | 100.0 | 0.141 | 0.09-0.60 | |
| 194 | 101.6 | 0.149 | 0.10-0.60 | |

*HEWLETT-PACKARD 175 OSCILLOSCOPE, TIME BASE CA. 5 μ SEC. ALL OTHER RECORDS FROM TEKTRONIX 454 OSCILLOSCOPE, TIME BASE CA. 1 μ SEC

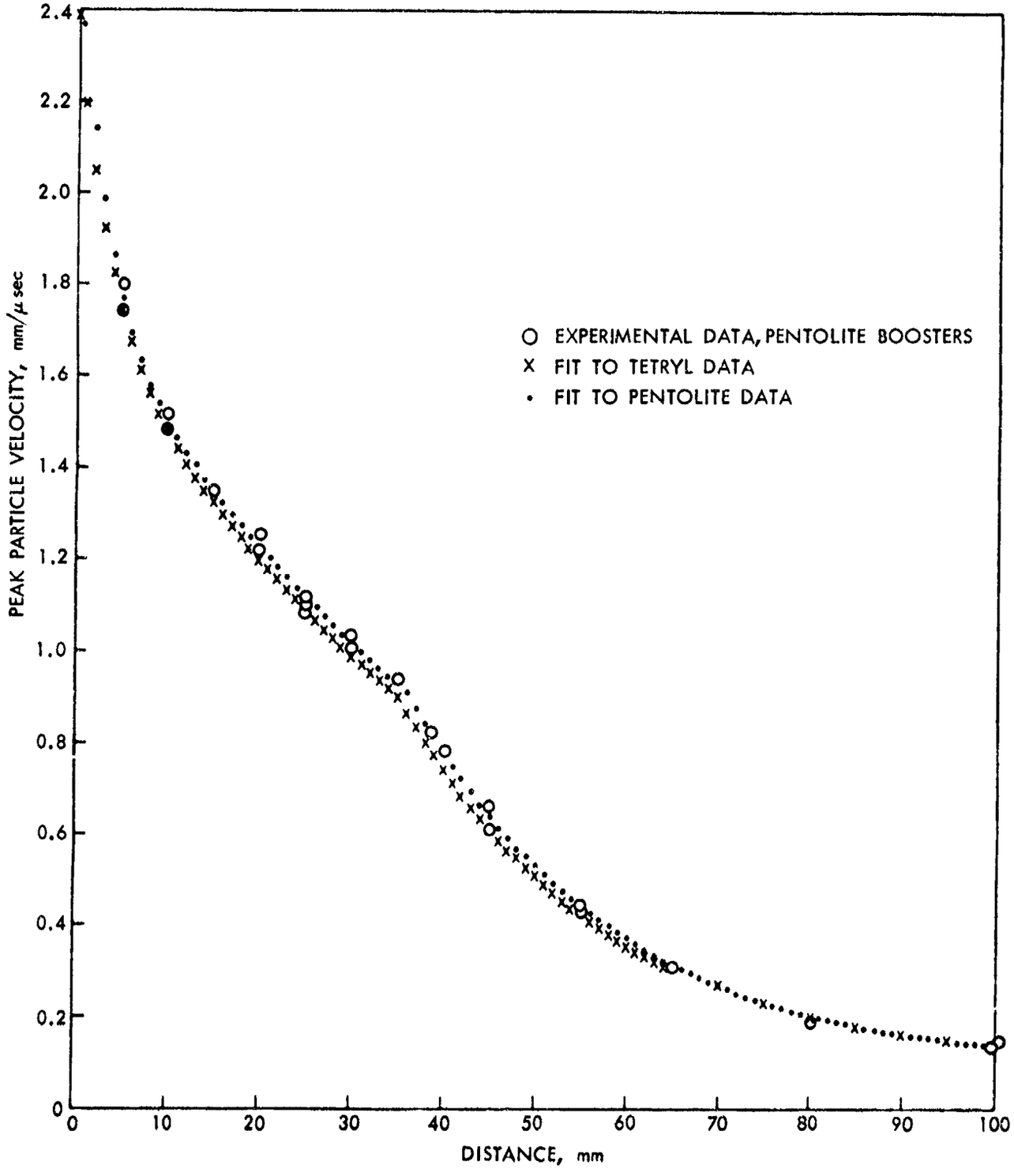


FIG. 13 EXPERIMENTAL RESULTS (PENTOLITE DONOR) COMPARED WITH RESULTS USING TETRYL DONOR

Our experience with the calibration for tetryl showed that we could expect erratic results close to, and at, the interface. At the interface, using a 51 mm long point initiated pentolite charge, we measured a particle velocity of 2.37 mm/μsec. We expect that results from a plane wave boosted (PWB) charge, using 25 mm of pentolite, would be greater than 2.37, as it was for tetryl; see above. The difference for tetryl was 0.28 mm/μsec. We add this increment to the value from Shot 286, Table 12, to obtain 2.65 mm/μsec as our interface value. As will be shown later, this gives us a reasonable calibration in the nominal region, $0 \leq x \leq 10$ mm.

The pentolite data are fitted with the double exponential, Equation (8), over the first 35 mm. The coefficients and their QME's are

| Coefficient | QME |
|---|---|
| 1.773 | 0.032 |
| 0.0184 | 0.0008 |
| 0.876 | 0.036 |
| 0.349 | 0.032 |

Residuals, which are given in Table 13, are all less than 0.03 in absolute value. The results of the fit are displayed in Figure 13 along with the fit to the tetryl data, and the experimental pentolite data. The fit appears to be adequate for interpolating over this part of the experimental data.

Data for pentolite at $x > 35$ mm are fitted with Equation (9) for which the coefficients, in order, and their QME's are

| Coefficient | QME |
|---|---|
| 0.0905 | 0.0075 |
| 4.0877 | 0.1588 |
| 0.0445 | 0.0012 |

The data and residuals are given in Table 14. In obtaining this fit, data for tetryl shots were included for $x \geq 80.0$ mm. Results of this fit are also shown in Figure 13. Note that the results for tetryl and pentolite converge for $x > 65$ mm. The slight differences in the two curves for $x > 65$ mm has no practical significance.

The two curves which represent the tetryl data cross at $x = 34.65$ mm; those representing pentolite, at 36 mm. When the two u,x curves are plotted on a very large scale and compared in the region $33 \leq x \leq 38$ mm, they are practically coincident after one is

Table 13

FIT TO PENTOLITE DATA x ≥ 36.0 mm
THE FUNCTION IS u=A exp(-Bx)+C exp(-Dx)

| x mm | u mm/μsec | u (Calculated) mm/μsec | Residuals mm/μsec |
|---|---|---|---|
| 0.00000 | 2.65000 | 2.64995 | .000 |
| 5.00000 | 1.80000 | 1.77021 | -.030 |
| 5.00000 | 1.74000 | 1.77021 | .030 |
| 10.00000 | 1.49400 | 1.50188 | .008 |
| 10.00000 | 1.51000 | 1.50188 | -.008 |
| 15.00000 | 1.35100 | 1.35019 | -.001 |
| 20.00000 | 1.25700 | 1.22804 | -.029 |
| 20.00000 | 1.22000 | 1.22804 | .008 |
| 25.00000 | 1.12000 | 1.11946 | -.001 |
| 25.00000 | 1.09000 | 1.11946 | .029 |
| 25.00000 | 1.11000 | 1.11946 | .009 |
| 30.00000 | 1.03800 | 1.02091 | -.017 |
| 30.00000 | 1.01000 | 1.02091 | .011 |
| 35.00000 | .94200 | .93112 | -.011 |

Table 14

FIT TO u VS x FOR PENTOLITE, x > 36.0 mm
THE FUNCTION IS u = A+B exp(-Cx)

| x mm | u mm/μsec | Weight | u (Calculated) mm/μsec | Residuals mm/μsec |
|---|---|---|---|---|
| 35.9 | .94200 | 2.0 | .95140 | .009 |
| 39.9 | .78600 | 2.0 | .78271 | -.003 |
| 45.0 | .66100 | 2.0 | .64214 | -.019 |
| 54.9 | .43100 | 2.0 | .44586 | .015 |
| 55.0 | .45100 | 2.0 | .44398 | -.007 |
| 65.1 | .31300 | 2.0 | .31599 | .003 |
| 80.0 | .20000 | 1.0 | .20668 | .007 |
| 80.0 | .19400 | 1.0 | .20668 | .013 |
| 80.1 | .19200 | 1.0 | .20616 | .014 |
| 89.8 | .16900 | 1.0 | .16561 | -.003 |
| 100.0 | .15100 | 1.0 | .13820 | -.013 |
| 100.0 | .14100 | 1.0 | .13820 | -.003 |
| 100.1 | .13500 | 1.0 | .13799 | .003 |
| 101.6 | .14800 | 1.0 | .13492 | -.013 |

shifted 1.35 mm, the difference found in location of the rarefaction waves for the two boosters. The fact that these locations differ has an interesting effect in our pressure calibration; this will be described in a later section.

In summary, the peak particle velocity in the PMMA attenuator of the LSGT for tetryl donor charges is given by

$$u = 1.7342 \exp(-0.01852\ x) + 0.6602 \exp(-0.2794\ x)$$

$$\text{for } x \leq 34.65 \text{ mm} \tag{10}$$

and

$$u = 0.0921 + 3.7038 \exp(-0.0435\ x) \text{ for } x > 34.65 \text{ mm}. \tag{11}$$

For pentolite donor charges, the results are

$$u = 1.7735 \exp(-0.01841\ x) + 0.8765 \exp(-0.3495\ x)$$

$$\text{for } x \leq 36 \text{ mm} \tag{12}$$

and

$$u = 0.0905 + 4.0877 \exp(-0.04451\ x) \text{ for } x > 36 \text{ mm}. \tag{13}$$

## 5. HUGONIOT OF PMMA

The end result of a gap calibration is a curve relating pressure to length of gap. The data presented in the two preceding sections could be used to provide the calibration. That is, for every value of x, we have values of u and U which define a value of P. Our data, however, are not entirely accurate as has been noted in previous sections. One way to examine the accuracy of the data is to study the Hugoniot curve which results by plotting U as a function of u. Then our results can be compared with results previously reported.

In the following discussion, we will be interested in pressures up to about 200 kbar. This is well below the phase change in PMMA which takes place between 212 and 276 kbar.[5]

Data on the Hugoniot of PMMA are available in the LLL compendium.[12] Most of the data that were available in 1965 were reviewed by Deal who noted that there was a large amount of scatter in the data.[13] He questioned the reproducibility of the material used in the experiments -- few authors gave a thorough characterization of the plastic used. Some of the scatter may well be due to differences in material.

Different techniques may also have contributed to the scatter. Since 1965, data have been acquired with new techniques on easily identified materials. The most accurate of these uses optical interferometry. Data taken with this technique at Sandia Laboratories in the range of 1-60 kbar[14,15] are used in the following as a check on our data. Results from General Motors[16] confirm the low pressure results reported by Sandia. Both sets of data are from samples cut from sheet stock of Plexiglas, produced by Rohm and Haas and designated Plexiglas II UVA, an ultraviolet absorbing grade. This is the same material which we use, the exception being that we use bar stock. As noted above, optical interferometry was used to study shocks in PMMA at Sandia. At General Motors, the data was acquired by the use of transducers, a method which is fairly new in this type of work. Because the data from Sandia extends over a greater range of pressures, we depend on them in the following discussion.

In these recent works, it has been shown that PMMA behaves in a complicated way when stressed by shock waves. It is generally conceded that the material is viscoelastic, and exhibits strain rate effects. There is also evidence that it behaves elastoplastically, at least when shocked to states above 25 kbar. One observation in reference (14) is that the shock velocity in an impacted piece of PMMA depends on the thickness of the piece. That is, even though there is no interaction of waves from the back of the projectile with the shock front in the sample, the shock velocity changes with distance. This is consistent with the observation that PMMA is a viscoelastic solid. Another observation is that, for example, impact by a PMMA projectile at a velocity of about 0.6 mm/μsec produces an abrupt rise of particle velocity to about 0.20 mm/μsec, followed by a slower rise to about 0.30 mm/μsec. The latter is equivalent to a pressure of about 12.3 kbar. This same type of behavior is observed at 19.4 kbar, while at 60 kbar the entire loading event is abrupt as it would be in a metal.[15] At low pressures, we really should not use the words "shock" and "Hugoniot" when we describe the response of PMMA when it is impacted by a projectile, or loaded by an explosive. For convenience, however, we will continue to use the familiar nomenclature. When we use the term "shock wave", we mean the entire loading process which takes place in PMMA whether or not it is entirely abrupt.

Our experimental relation between U and u is shown in Figure 14. This is a graph of the data presented in the previous two sections of this report for pentolite donor charges. Each point in the graph corresponds to a value of x, the distance from the donor explosive. Some representative values of x are indicated on the graph as an aid in the following discussion. Our results are not linear, even at the high pressure end of our set of data. A consequence of this is that extrapolation is more of a problem than it would be if our data were linear at the higher pressures. A procedure for extrapolating will be discussed below. Curvature at low pressure is expected. Data acquired previously at NOL showed that PMMA had an anomolous Hugoniot.[4] Data from SRI,[17] Sandia Laboratories[14,15] and General Motors[16] confirm the observation of this behavior.

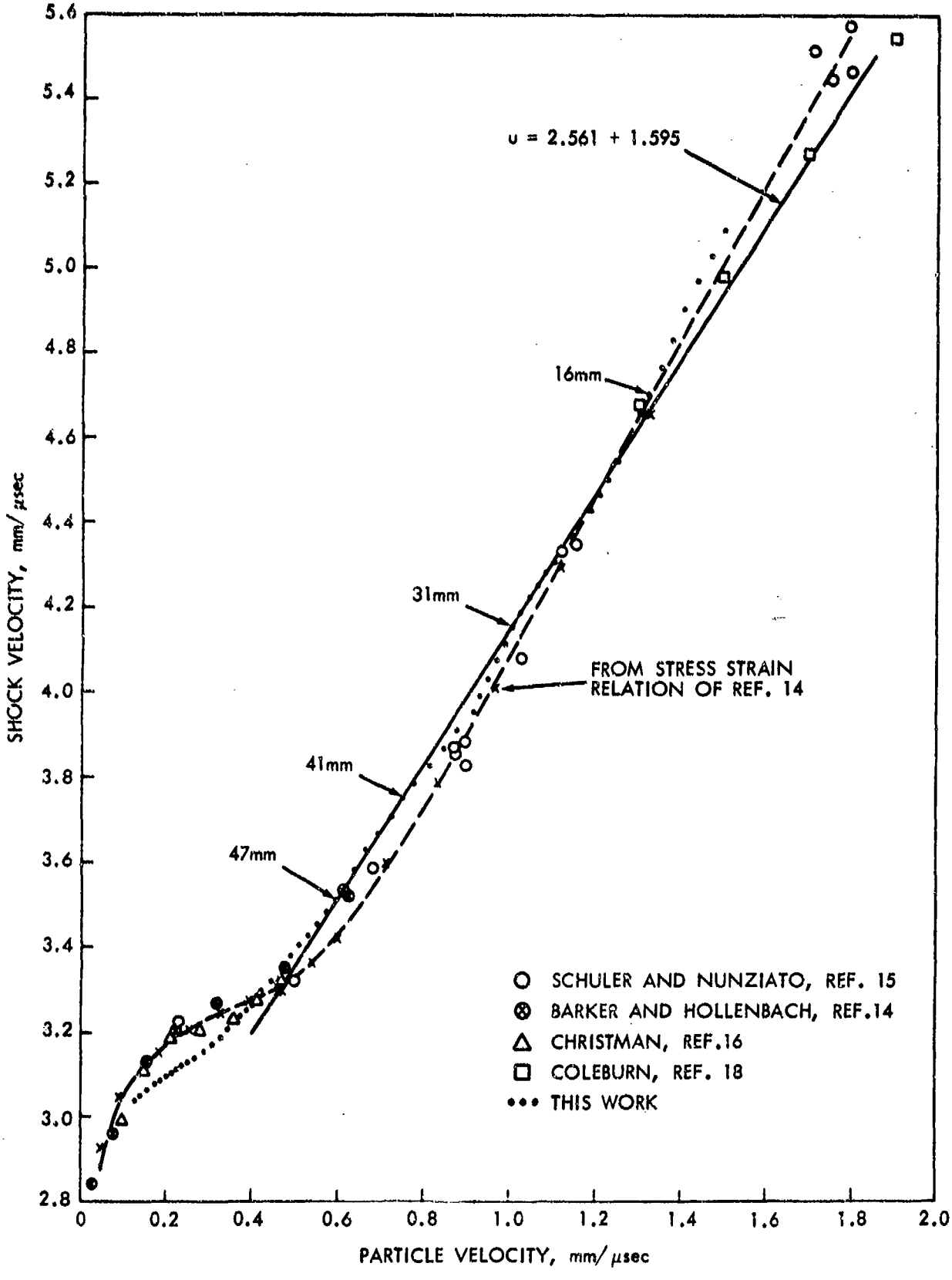


FIG. 14 HUGONIOT OF PMMA

Schuler and Nunziato[14] have an expression which fits their data and that of Barker and Hollenbach.[13] They chose to relate the stress to the strain rather than to relate shock and particle velocities. Their expression is

$$\sigma = 87.066\varepsilon + 858.71\varepsilon^2 - 7063.23\varepsilon^3 + 22040.8\varepsilon^4 \qquad (14)$$

where $\sigma$ is the stress in kbars and $\varepsilon$ is the strain (engineering). Using the relation

$$\varepsilon = 1 - V/V_0 \qquad (15)$$

where V is the specific volume and $V_0$ is the specific volume at ambient stress, and the Hugoniot relations, there results,

$$\varepsilon = u/U \qquad (16)$$

$$\sigma = \rho_0 uU \qquad (17)$$

The above relations permit the construction of a u,U curve from the Sandia relation, Equation (14). With this representation, we have a continuous curve covering about 60 kbar of the PMMA Hugoniot. Curvature at low pressure is more pronounced than it is in our data, see Figure 14. This curvature is substantiated by the results from General Motors[16] which are also shown in Figure 14. Schuler and Nunziato[15] did not use the two points from Barker and Hollenbach[14] for which u is about 0.61 and 0.625 mm/μsec in their determination of the constants in Equation (14). Their reason for not using these data is that they were obtained from experiments in which the projectiles were tungsten carbide. These experiments could not be analysed as satisfactorily as the other experiments in which the projectiles were PMMA. Hence they decided to ignore these two points rather than to take a chance on less than satisfactory results.

The curve shown in Figure 14 for the Schuler and Nunziato[15] data was constructed from "equilibrium" values of particle velocity. In some instances, a time interval as long as one μsec was required for the instantaneous u to build up to its higher equilibrium value. Since this build-up time is often greater than our time of measurement of u, there is some question of the applicability of the equilibrium curve to our data. To be sure, when the Liddiard[4] data (U, 1/2 $u_{fs}$) are corrected to U, u data by means of Figure 12, they fall on the equilibrium curve. However, this may be a fortuitous agreement.

The difference between the curve derived from Equation (14) and the curve which represents our data is small. This is shown in

Figure 15 where the difference in pressure between the two representations is plotted as a function of x. In constructing this plot, we used the U vs x data reported in Section 3 and the u vs x of Section 4 of this report for pentolite donors. Pressure, based on the Sandia curve, is also shown on the plot. The difference in pressure is less than a kbar except for $x < 13$ mm. Hence either representation could be used in our calibration over the range of pressure up to about 80 kbar.

We need to extend our Hugoniot representation to about 200 kbar so we can obtain a nominal calibration for the LSGT for small gaps. Examining Figure 14 shows that we could use the Sandia curve for the extrapolation -- it reproduces our data to within experimental error up to a particle velocity of 1.5 mm/μsec (90 kbar). This agreement may be fortuitious as will be demonstrated in the following. Some of the data reported by Coleburn[18] are shown in Figure 14; these indicate that the extrapolated Sandia curve is too steep. The slope of the curve is about 1.9 for $0.9 \leq u \leq 1.9$ mm/μsec. Coleburn fitted his data with a quadratic which has a slope of about 1.47 at $u = 1.5$. Values of the slope of straight line fits to PMMA Hugoniot data in this range have been reported as 1.61[3,5] and 1.69.[4] It was decided not to risk using the extrapolation with the steep slope, so we tried finding a straight line through a part of our data which could be used for extrapolation. Placing a straight edge on the plot shows that a straight line can be drawn through two subsets of the data. These subsets are for $0.595 \leq u \leq 0.749$ and $1.002 \leq u \leq 1.324$. Ignoring the non-linearity of the intermediate data is justified as follows. Those data which sag below the straight line come from measurements for x between 31 and 41 mm. It must be recalled that the u vs x curve was treated so that a cusp appeared at about 35 mm. If wave interaction in the cylinder of PMMA can produce this anomolous behavior in the particle velocity curve, it can surely produce similar behavior in the shock velocity. We may have smoothed the x,t data and the U,x data so that we suppressed some of the effects of wave interaction on the results. We do observe a hump in the U,x curve at about 35 mm. Treated differently, this hump might look more like the cusp which appears in our treatment of the particle velocity. The results might also eliminate the sag in our U,u curve. Furthermore, the greatest divergences in shock velocities were observed at 35 and 40 mm, see Table 6. These considerations do not prove that those points which we ignore are really in error -- they do point to the possibility.

The data at the top end of our curve ($u > 1.324$) come from locations within 16 mm of the donor explosive. In this region the shock velocity changes rapidly, with the result that the streak camera records are difficult to differentiate. One of the two records gave very poor data over the first 8 mm. Here too, a reasonable case is available for ignoring the nonlinear data at the high pressure end of our curve. The fact that nonlinearity in this region of the U,u curve has not been reported by other investigators has also been considered.

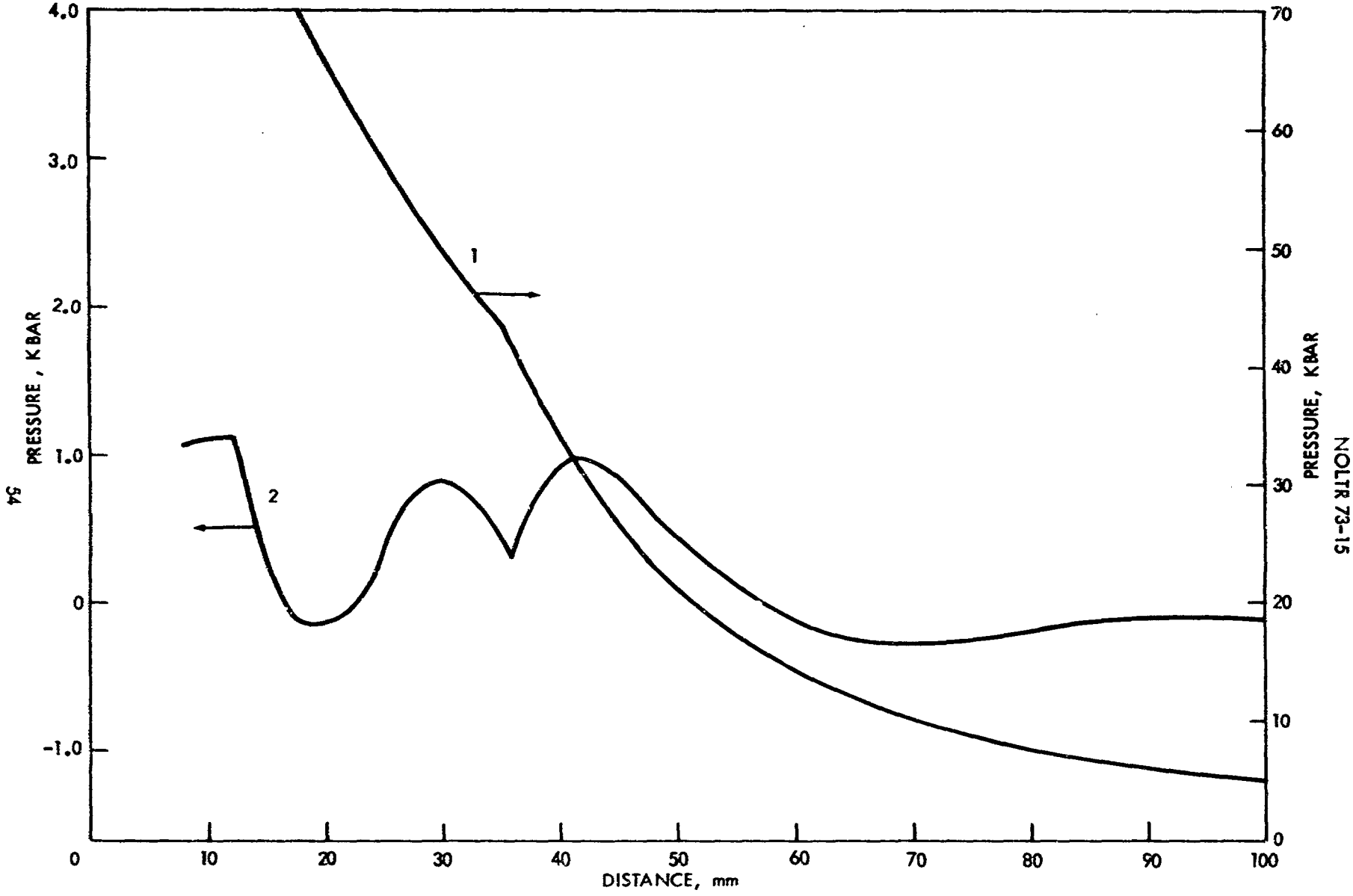


FIG. 15 PRESSURE VS DISTANCE (PENOLITE DONORS)
CURVE 1: PRESSURE USING EMV GAGE RESULTS OF FIG. 13 AND HUGONIOT RELATION OF FIG. 14 BASED ON REF. 14 STRESS STRAIN RELATION (EQ 14)
CURVE 2: DIFFERENCE IN PRESSURE FROM CURVE 1 AND PRESSURE CALCULATED USING EMV GAGE RESULTS OF FIG. 13 AND EXPERIMENTAL HUGONIOT RELATION OF FIG. 14



NOLTR 73-15

The line mentioned above is represented by

$$U = 2.561 + 1.595\ u. \tag{18}$$

In previous work with tetryl donor charges the coefficients were found to be 2.57 and 1.61 respectively.[3] Considering all the possibilities of errors in measurements and in interpretation, the two results are in good agreement.

At low pressures (low u and U), we are at the other extreme of our experimental measurements. There seems little doubt that the Sandia[14,15] measurements should be more accurate than any we can make. Consequently we have fitted the Sandia data, shown in Table 15, with a cubic constrained to become tangent to the straight line of Equation (18). Thus our final selection for the Hugoniot is

$$U = 2.7228 + 4.0667u - 10.9051u^2 + 10.6912u^3,\ 0.03 \leq u \leq 0.5363 \tag{19}$$

and

$$U = 2.561 + 1.595u,\ u > 0.5363. \tag{18'}$$

Figure 16 shows Equations (19) and (18') as the solid line curve, the Sandia data from which Equation (19) was obtained, and the low pressure U,u data of the present work. The latter, discarded in selecting the Hugoniot, lead to differences of < 0.3 kbar (at the same x or u value) in the pressure computed with the Hugoniot of Equation (19) and those computed with the discarded U,u data (see Figure 15).

## 6. PRESSURE-DISTANCE CALIBRATION FOR THE LSGT

We now have the particle velocity vs distance relation for the PMMA attenuator of the LSGT in analytical form for both tetryl and pentolite donor charges (Section 4). These constitute our primary calibration curves for reasons presented in the error analysis. In addition, we have analytical expressions relating the particle and shock velocities along the PMMA Hugoniot (Equations (18') and (19) of the previous section). From the above combination we can calculate the pressure in the attenuator at any distance from either donor charge by using

$$P = \rho_0\ u\ U \tag{20}$$

where $\rho_0$ is the density of PMMA, taken to be 1.185 g/cc. Table 16 gives the computed pressures at 5-10 mm intervals in x.

Table 15

CUBIC FIT TO LOW PRESSURE
HUGONIOT DATA FOR PMMA
(SANDIA CORPORATION DATA)

| u mm/μsec | U mm/μsec | U (Calculated) mm/μsec | Residual mm/μsec |
|---|---|---|---|
| .03045 | 2.843 | 2.83685 | -0.006 |
| .03066 | 2.844 | 2.83757 | -0.006 |
| .07555 | 2.968 | 2.97243 | 0.004 |
| .07580 | 2.959 | 2.97308 | 0.014 |
| .1542 | 3.127 | 3.12981 | 0.003 |
| .1545 | 3.130 | 3.13025 | 0.000 |
| .2250 | 3.199 | 3.20754 | 0.009 |
| .3206 | 3.268 | 3.25804 | -0.009 |
| .3196 | 3.268 | 3.25767 | -0.010 |
| .4801 | 3.349 | 3.34476 | -0.004 |
| .4805 | 3.342 | 3.34516 | 0.003 |
| .228 | 3.22 | 3.20986 | -0.010 |
| .500 | 3.32 | 3.36629 | -0.046 |

NOTE: Last two points from Schuler and Nunziato; remainder from Barker and Hollenbach.

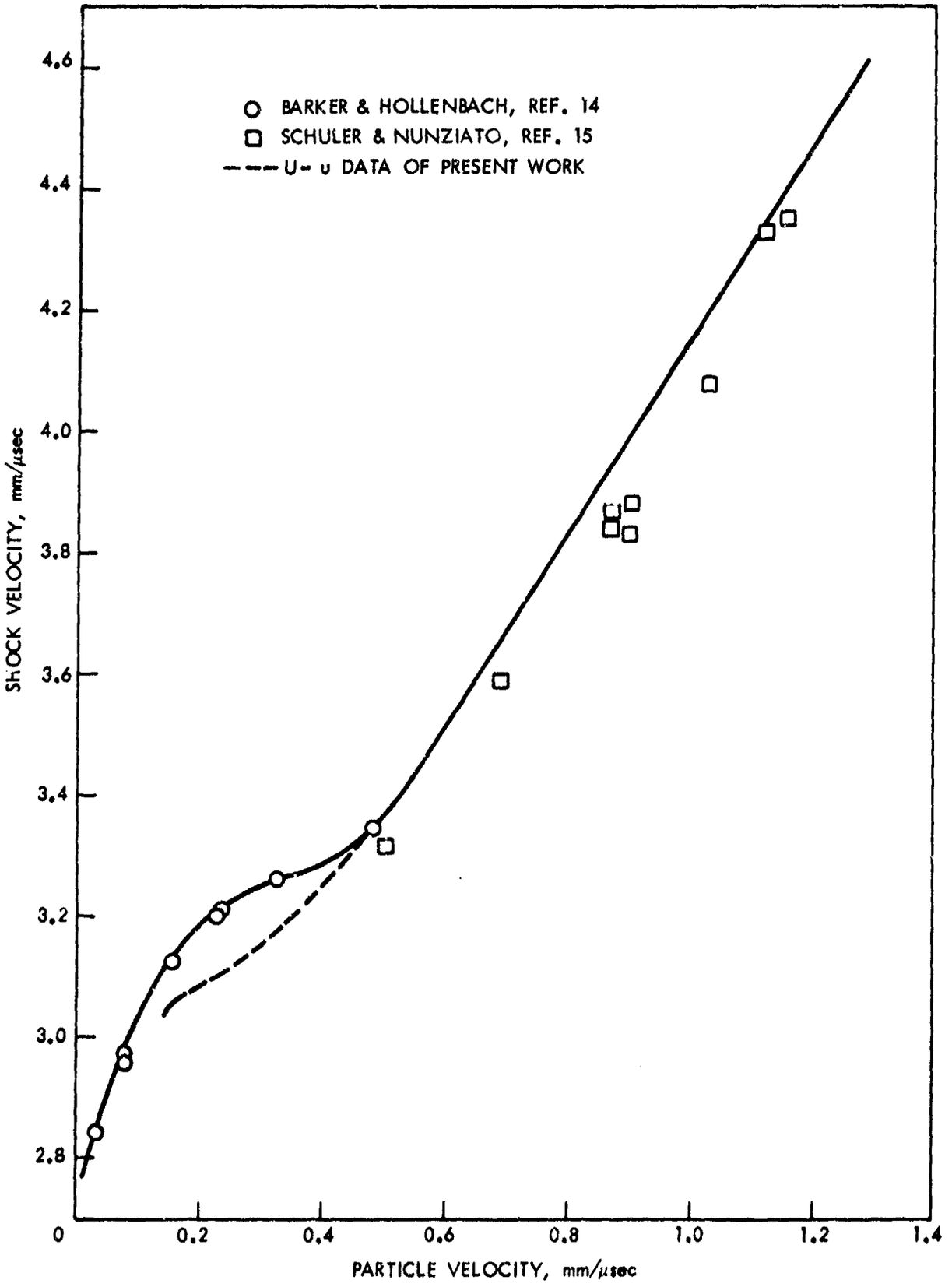


FIG. 16 HUGONIOT SELECTED FOR PMMA

Table 16

PRESSURE-DISTANCE DATA FROM CALIBRATIONS OF THIS REPORT

| x, mm | P, Kbar | |
|---|---|---|
| | Tetryl | Pentolite |
| 0 | 181.0 | 213.1 |
| 5 | 110.4 | 113.0 |
| 10 | 86.4 | 88.2 |
| 15 | 73.3 | 75.4 |
| 20 | 63.6 | 65.8 |
| 25 | 55.7 | 57.7 |
| 30 | 48.9 | 50.7 |
| 35 | 42.6 | 44.6 |
| 40 | 32.9 | 35.1 |
| 45 | 25.8 | 27.3 |
| 50 | 20.6 | 21.5 |
| 55 | 16.9 | 17.5 |
| 60 | 14.1 | 14.5 |
| 70 | 10.3 | 10.4 |
| 80 | 7.8 | 7.8 |
| 90 | 6.2 | 6.1 |
| 100 | 5.2 | 5.1 |

Since the unit of length used in the gap test is the thickness of a card (0.01 inch), it is convenient to tabulate the pressure at one card intervals. This can easily be done by use of a digital computer; Tables 17 and 18 contain the final calibration values for tetryl and pentolite donors, respectively. The gap length in these tables is the sum of the number in the left column and the number at the top of a column. Each table gives P for zero through 400 cards. Although pressure is reported to 0.1 kbar, the fractional part is not significant.

A rigorous analysis of the possible error in the pressure has not been carried out. An analysis of the error expected in the measured particle velocity gives an estimate of ±6% in an individual determination (see Appendix). Replicate measurements over the range of 0.2-1.5 mm/μsec show differences of 4% or less and, therefore, suggest the ±6% is probably pessimistic; however, replicates at 0.15 mm/μsec show a difference of 11%. The error in P must be at least as large as the error in u; it is probably somewhat larger because of any error in the Hugoniot we have selected.

As in the case of particle velocity, at any given $x \geq 10$ mm (39 cards), the difference in pressure, obtained by tetryl and pentolite loading, is not experimentally significant. The numerical difference (values of Table 18 minus those of Table 17) runs from 32 kbar at x = 0 cards to 0 at 400 cards. The maximum percentage difference, in the range $x \geq 10$ cards, is about 7% (2.6 kbar) and occurs at x of 140-150 cards. This is the direct result of a similar maximum difference in particle velocity caused by differences in the location of the rarefaction waves (cusps in the fitted u-x curves) in the two cases.* It was remarked in Section 4, that shifting one of the u-x curves by 1.35 mm (or about 5 cards) resulted in coincidence of the two curves. In agreement with this, Tables 17 and 18 show that the pressure at x cards for tetryl is the same (±0.1 kbar) as that at (x + 5) cards for pentolite in the range of 70-230 cards. At greater attenuations, of course, the pressure is the same (±0.1 kbar) for the same number of cards; this is true for the range 260-400 cards.

In earlier work,[1] two pairs of tests were carried out in the region 70-230 cards. For the same acceptor and different donors (tetryl and pentolite), the pairs showed differences of one and zero cards in the two respective 50% gaps. This is not the 5 card difference expected, but it indicates the same pressure amplitude within the expected error. The expected error is just too large to resolve the effect of different pressure profiles of the same amplitude.

---

*Use of our U,u data or the Sandia equilibrium U,u data instead of the Hugoniot we have chosen has no effect on the size of this difference. The Sandia data result in lower absolute pressure values; at $x \geq 80$ cards, the maximum difference is 1.5 kbar and 1 kbar, respectively, for tetryl and pentolite.

TABLE 17

CALIBRATION OF NOL LARGE SCALE GAP TEST FOR TETRYL

NUMBER OF CARDS IN GAP IS SUM OF A NUMBER IN FIRST ROW AND A NUMBER IN THE FIRST COLUMN. ONE CARD IS 0.01 INCH. PRESSURE IN KILOBARS.

| | 0 | 1 | 2 | 3 | 4 | 5 | 6 | 7 | 8 | 9 |
|---|---|---|---|---|---|---|---|---|---|---|
| 0 | 181.0 | 174.6 | 168.7 | 163.2 | 158.1 | 153.4 | 149.0 | 144.9 | 141.0 | 137.6 |
| 10 | 134.1 | 131.0 | 128.0 | 125.3 | 122.7 | 120.2 | 117.9 | 115.7 | 113.7 | 111.7 |
| 20 | 109.9 | 108.1 | 106.4 | 104.8 | 103.3 | 101.9 | 100.5 | 99.2 | 97.9 | 96.7 |
| 30 | 95.5 | 94.4 | 93.3 | 92.3 | 91.3 | 90.3 | 89.4 | 88.5 | 87.6 | 86.7 |
| 40 | 85.9 | 85.1 | 84.3 | 83.6 | 82.8 | 82.1 | 81.4 | 80.7 | 80.0 | 79.3 |
| 50 | 78.7 | 78.0 | 77.4 | 76.8 | 76.2 | 75.6 | 75.0 | 74.4 | 73.9 | 73.3 |
| 60 | 72.8 | 72.2 | 71.7 | 71.2 | 70.6 | 70.1 | 69.6 | 69.1 | 68.6 | 68.1 |
| 70 | 67.6 | 67.2 | 66.7 | 66.2 | 65.8 | 65.3 | 64.8 | 64.4 | 64.0 | 63.5 |
| 80 | 63.1 | 62.6 | 62.2 | 61.8 | 61.4 | 61.0 | 60.5 | 60.1 | 59.7 | 59.3 |
| 90 | 58.9 | 58.5 | 58.1 | 57.7 | 57.4 | 57.0 | 56.6 | 56.2 | 55.8 | 55.5 |
| 100 | 55.1 | 54.7 | 54.4 | 54.0 | 53.7 | 53.3 | 53.0 | 52.6 | 52.3 | 51.9 |
| 110 | 51.6 | 51.2 | 50.9 | 50.6 | 50.2 | 49.9 | 49.6 | 49.3 | 49.0 | 48.6 |
| 120 | 48.3 | 48.0 | 47.7 | 47.4 | 47.1 | 46.8 | 46.5 | 46.2 | 45.9 | 45.6 |
| 130 | 45.3 | 45.0 | 44.7 | 44.4 | 44.1 | 43.9 | 43.6 | 43.1 | 42.5 | 41.9 |
| 140 | 41.4 | 40.8 | 40.3 | 39.8 | 39.2 | 38.7 | 38.2 | 37.7 | 37.2 | 36.7 |
| 150 | 36.3 | 35.8 | 35.3 | 34.9 | 34.4 | 34.0 | 33.6 | 33.1 | 32.7 | 32.3 |
| 160 | 31.9 | 31.5 | 31.1 | 30.7 | 30.3 | 30.0 | 29.6 | 29.2 | 28.9 | 28.5 |
| 170 | 28.2 | 27.8 | 27.5 | 27.2 | 26.8 | 26.5 | 26.2 | 25.9 | 25.6 | 25.3 |
| 180 | 25.0 | 24.7 | 24.4 | 24.1 | 23.8 | 23.5 | 23.3 | 23.0 | 22.7 | 22.5 |
| 190 | 22.2 | 21.9 | 21.7 | 21.5 | 21.2 | 21.0 | 20.7 | 20.5 | 20.3 | 20.1 |
| 200 | 19.9 | 19.7 | 19.5 | 19.3 | 19.1 | 18.9 | 18.7 | 18.5 | 18.3 | 18.1 |
| 210 | 18.0 | 17.8 | 17.6 | 17.4 | 17.3 | 17.1 | 17.0 | 16.8 | 16.6 | 16.5 |
| 220 | 16.3 | 16.2 | 16.0 | 15.9 | 15.7 | 15.6 | 15.5 | 15.3 | 15.2 | 15.1 |
| 230 | 14.9 | 14.8 | 14.7 | 14.5 | 14.4 | 14.3 | 14.2 | 14.0 | 13.9 | 13.8 |
| 240 | 13.7 | 13.6 | 13.5 | 13.3 | 13.2 | 13.1 | 13.0 | 12.9 | 12.8 | 12.7 |
| 250 | 12.6 | 12.5 | 12.4 | 12.3 | 12.2 | 12.1 | 12.0 | 11.9 | 11.8 | 11.7 |
| 260 | 11.6 | 11.5 | 11.4 | 11.3 | 11.3 | 11.2 | 11.1 | 11.0 | 10.9 | 10.8 |
| 270 | 10.7 | 10.7 | 10.6 | 10.5 | 10.4 | 10.3 | 10.3 | 10.2 | 10.1 | 10.0 |
| 280 | 10.0 | 9.9 | 9.8 | 9.7 | 9.7 | 9.6 | 9.5 | 9.5 | 9.4 | 9.3 |
| 290 | 9.3 | 9.2 | 9.1 | 9.1 | 9.0 | 8.9 | 8.9 | 8.8 | 8.7 | 8.7 |
| 300 | 8.6 | 8.6 | 8.5 | 8.4 | 8.4 | 8.3 | 8.3 | 8.2 | 8.2 | 8.1 |
| 310 | 8.1 | 8.0 | 8.0 | 7.9 | 7.8 | 7.8 | 7.7 | 7.7 | 7.6 | 7.6 |
| 320 | 7.6 | 7.5 | 7.5 | 7.4 | 7.4 | 7.3 | 7.3 | 7.2 | 7.2 | 7.1 |
| 330 | 7.1 | 7.1 | 7.0 | 7.0 | 6.9 | 6.9 | 6.8 | 6.8 | 6.8 | 6.7 |
| 340 | 6.7 | 6.7 | 6.6 | 6.6 | 6.5 | 6.5 | 6.5 | 6.4 | 6.4 | 6.4 |
| 350 | 6.3 | 6.3 | 6.3 | 6.2 | 6.2 | 6.2 | 6.1 | 6.1 | 6.1 | 6.0 |
| 360 | 6.0 | 6.0 | 5.9 | 5.9 | 5.9 | 5.9 | 5.8 | 5.8 | 5.8 | 5.7 |
| 370 | 5.7 | 5.7 | 5.7 | 5.6 | 5.6 | 5.6 | 5.6 | 5.5 | 5.5 | 5.5 |
| 380 | 5.5 | 5.4 | 5.4 | 5.4 | 5.4 | 5.3 | 5.3 | 5.3 | 5.3 | 5.3 |
| 390 | 5.2 | 5.2 | 5.2 | 5.2 | 5.1 | 5.1 | 5.1 | 5.1 | 5.1 | 5.0 |
| 400 | 5.0 | | | | | | | | | |

NOTE--RESULTS ARE [illegible]

TABLE 18

CALIBRATION OF NOL CARDS GAP TEST FOR LOT 718 PENTOLITE

NUMBER OF CARDS IN GAP IS SUM OF A NUMBER IN FIRST ROW AND A NUMBER IN THE FIRST COLUMN. ONE CARD IS 0.01 INCH. PRESSURE IN KILOBARS.

| | 0 | 1 | 2 | 3 | 4 | 5 | 6 | 7 | 8 | 9 |
|---|---|---|---|---|---|---|---|---|---|---|
| 0 | 211.1 | 202.5 | 192.9 | 186.2 | 176.3 | 169.2 | 162.7 | 156.8 | 151.4 | 146.9 |
| 10 | 142.0 | 137.9 | 134.1 | 130.6 | 127.3 | 124.3 | 121.6 | 119.0 | 116.6 | 114.4 |
| 20 | 112.3 | 110.4 | 108.6 | 106.8 | 105.2 | 103.7 | 102.2 | 100.9 | 99.6 | 98.3 |
| 30 | 97.2 | 96.0 | 94.9 | 93.9 | 92.9 | 92.0 | 91.1 | 90.2 | 89.3 | 88.5 |
| 40 | 87.7 | 86.9 | 86.2 | 85.4 | 84.7 | 84.0 | 83.3 | 82.6 | 82.0 | 81.3 |
| 50 | 80.7 | 80.1 | 79.5 | 78.9 | 78.3 | 77.7 | 77.1 | 76.6 | 76.0 | 75.5 |
| 60 | 74.9 | 74.4 | 73.9 | 73.4 | 72.8 | 72.3 | 71.8 | 71.3 | 70.8 | 70.3 |
| 70 | 69.8 | 69.3 | 68.9 | 68.4 | 67.9 | 67.5 | 67.0 | 66.6 | 66.1 | 65.7 |
| 80 | 65.2 | 64.8 | 64.3 | 63.9 | 63.5 | 63.1 | 62.6 | 62.2 | 61.8 | 61.4 |
| 90 | 61.0 | 60.6 | 60.2 | 59.8 | 59.4 | 59.0 | 58.6 | 58.2 | 57.8 | 57.4 |
| 100 | 57.1 | 56.7 | 56.3 | 55.9 | 55.6 | 55.2 | 54.9 | 54.5 | 54.1 | 53.8 |
| 110 | 53.4 | 53.1 | 52.7 | 52.4 | 52.1 | 51.7 | 51.4 | 51.0 | 50.7 | 50.4 |
| 120 | 50.1 | 49.7 | 49.4 | 49.1 | 48.8 | 48.5 | 48.2 | 47.8 | 47.5 | 47.2 |
| 130 | 46.9 | 46.6 | 46.3 | 46.0 | 45.7 | 45.4 | 45.2 | 44.9 | 44.6 | 44.3 |
| 140 | 44.0 | 43.7 | 43.4 | 43.2 | 42.9 | 42.6 | 42.3 | 42.0 | 41.8 | 41.5 |
| 150 | 41.2 | 41.0 | 40.7 | 40.4 | 40.2 | 39.9 | 39.7 | 39.4 | 39.2 | 38.9 |
| 160 | 38.7 | 38.4 | 38.2 | 37.9 | 37.7 | 37.5 | 37.2 | 37.0 | 36.8 | 36.5 |
| 170 | 36.3 | 36.1 | 35.9 | 35.7 | 35.4 | 35.2 | 35.0 | 34.8 | 34.6 | 34.4 |
| 180 | 34.2 | 34.0 | 33.8 | 33.6 | 33.4 | 33.2 | 33.0 | 32.8 | 32.6 | 32.4 |
| 190 | 32.2 | 32.0 | 31.8 | 31.6 | 31.4 | 31.2 | 31.0 | 30.8 | 30.6 | 30.4 |
| 200 | 30.2 | 30.0 | 29.8 | 29.6 | 29.4 | 29.2 | 29.0 | 28.8 | 28.6 | 28.4 |
| 210 | 28.2 | 28.0 | 27.8 | 27.6 | 27.4 | 27.2 | 27.0 | 26.8 | 26.6 | 26.4 |
| 220 | 26.2 | 26.0 | 25.8 | 25.6 | 25.4 | 25.2 | 25.0 | 24.8 | 24.6 | 24.4 |
| 230 | 24.2 | 24.0 | 23.8 | 23.6 | 23.4 | 23.2 | 23.0 | 22.8 | 22.6 | 22.4 |
| 240 | 22.2 | 22.0 | 21.8 | 21.6 | 21.4 | 21.2 | 21.0 | 20.8 | 20.6 | 20.4 |
| 250 | 20.2 | 20.0 | 19.8 | 19.6 | 19.4 | 19.2 | 19.0 | 18.8 | 18.6 | 18.4 |
| 260 | 18.2 | 18.0 | 17.8 | 17.6 | 17.4 | 17.2 | 17.0 | 16.8 | 16.6 | 16.4 |
| 270 | 16.2 | 16.0 | 15.8 | 15.6 | 15.4 | 15.2 | 15.0 | 14.8 | 14.6 | 14.4 |
| 280 | 14.2 | 14.0 | 13.8 | 13.6 | 13.4 | 13.2 | 13.0 | 12.8 | 12.6 | 12.4 |
| 290 | 12.2 | 12.0 | 11.8 | 11.6 | 11.4 | 11.2 | 11.0 | 10.8 | 10.6 | 10.4 |
| 300 | 10.2 | 10.0 | 9.8 | 9.6 | 9.4 | 9.2 | 9.0 | 8.8 | 8.6 | 8.4 |
| 310 | 8.2 | 8.0 | 7.8 | 7.6 | 7.4 | 7.2 | 7.0 | 6.8 | 6.6 | 6.4 |
| 320 | 6.2 | 6.0 | 5.8 | 5.6 | 5.4 | 5.2 | 5.0 | 4.8 | 4.6 | 4.4 |
| 330 | 4.2 | 4.0 | 3.8 | 3.6 | 3.4 | 3.2 | 3.0 | 2.8 | 2.6 | 2.4 |
| 340 | 2.2 | 2.0 | 1.8 | 1.6 | 1.4 | 1.2 | 1.0 | 0.8 | 0.6 | 0.4 |
| 350 | 0.2 | 0.0 | | | | | | | | |

Table 19 has been prepared so that the two calibrations just described can be compared with the old tetryl calibration. Columns 1 and 2 of Table 19 are from Column 1 of Tables 17 and 18 respectively. That is, the calibrated pressure is given at 10 card intervals in Table 19. Column 3 represents the previous calibration for tetryl; an interpolation was performed on the previously reported results. The difference at zero gap is due to the way the nominal part of the calibration was done. In both the new calibrations, an EMV gage was used to measure and estimate the particle velocity at the explosive/PMMA interface. In the old tetryl calibration, the interface value was computed, using C-J parameters for the explosive gases. This resulted in a lower interface pressure than that which is produced in the explosive event. If we had used values for the parameters describing the state in the explosive gases which is appropriate to the von Neumann spike, our previous results would have been closer to the present ones. All this is to say that the new nominal values are better approximations than those published previously.

At 20 cards, the three calibrations are remarkably close; the new value for tetryl is slightly smaller than the old value and the value for pentolite is slightly greater, as expected. At the end of the nominal range (39 cards), the new value for tetryl is about 1 kbar larger than the old. The difference increases to a maximum value of 7 kbar at 140 cards, then decreases to 2.6 kbar at 200 cards. Thereafter it continues to decrease to 0.4 kbar at 320 cards. From 330-400 cards, the two values are the same ±0.2 kbar.

The maximum difference in pressure (26 kbar at x = 0) amounts to about 17% change; the maximum percentage difference is 20% at 140 cards. The uncertainty in the earlier calibration was estimated as ±10%; in the present one it is ±16%. The maximum change is therefore about the sum of the two uncertainties.

Despite the fact that the new results for tetryl are in some ranges significantly larger than the early ones, the two (old and new) P vs x curves do not cross. Therefore the relative ranking of explosives by gap sensitivity will not be changed although the 50% pressures ($P_0$) will be, in some cases. The same situation also exists for the old and new calibrations with pentolite.

The results for pentolite are consistently (but not always significantly) greater than those of the tetryl calibration except at large attenuations. For practical purposes, we can use the same calibration (P vs x) curve for both tetryl and pentolite at x > 200 cards.

## Table 19

## COMPARISON OF PRESSURE CALIBRATION

| Gap Length Cards | Pressure, Kbar | | |
|---|---|---|---|
| | Tetryl | Pentolite | Tetryl Old |
| 0 | 181.0 | 213.1 | 154.8 |
| 10 | 134.1 | 142.0 | 130.3 |
| 20 | 109.9 | 112.3 | 111.0 |
| 30 | 95.5 | 97.2 | 96.3 |
| 40 | 85.9 | 87.7 | 85.0 |
| 50 | 78.7 | 80.7 | 76.3 |
| 60 | 72.8 | 74.9 | 69.3 |
| 70 | 67.6 | 69.8 | 63.4 |
| 80 | 63.1 | 65.2 | 58.2 |
| 90 | 58.9 | 61.0 | 53.7 |
| 100 | 55.1 | 57.1 | 49.5 |
| 110 | 51.6 | 53.4 | 45.6 |
| 120 | 48.3 | 50.1 | 41.9 |
| 130 | 45.3 | 46.9 | 38.1 |
| 140 | 41.4 | 44.0 | 34.4 |
| 150 | 36.3 | 38.9 | 30.8 |
| 160 | 31.9 | 34.0 | 27.4 |
| 170 | 28.2 | 29.9 | 24.3 |
| 180 | 25.0 | 26.3 | 21.6 |
| 190 | 22.2 | 23.3 | 19.3 |
| 200 | 19.9 | 20.7 | 17.3 |
| 210 | 18.0 | 18.6 | 15.7 |
| 220 | 16.3 | 16.9 | 14.3 |
| 230 | 14.9 | 15.3 | 13.1 |
| 240 | 13.7 | 14.0 | 12.1 |
| 250 | 12.6 | 12.9 | 11.2 |
| 260 | 11.6 | 11.8 | 10.3 |
| 270 | 10.7 | 10.9 | 9.6 |
| 280 | 10.0 | 10.1 | 9.0 |
| 290 | 9.3 | 9.3 | 8.4 |
| 300 | 8.6 | 8.7 | 8.0 |
| 310 | 8.1 | 8.1 | 7.5 |
| 320 | 7.6 | 7.6 | 7.2 |
| 330 | 7.1 | 7.1 | 6.9 |
| 340 | 6.7 | 6.7 | 6.6 |
| 350 | 6.3 | 6.3 | 6.3 |
| 360 | 6.0 | 6.0 | 6.1 |
| 370 | 5.7 | 5.7 | 5.9 |
| 380 | 5.5 | 5.4 | 5.6 |
| 390 | 5.2 | 5.2 | 5.4 |
| 400 | 5.0 | 5.0 | |

## REFERENCES


1. D. Price, "Calibration of the NOL Large Scale Gap Test with a Pentolite Donor II", NOLTR 70-25, 17 Mar 1970.

2. D. D. Keough and J. Y. Wong, "Variation of the Shock Piezoresistance Coefficient of Manganin as a Function of Deformation", J. Appl. Physics, 41, 3508 (1970).

3. D. Price and T. P. Liddiard, Jr., "The Small Scale Gap Test: Calibration and Comparison with the Large Scale Gap Test", NOLTR 66-87, 7 Jul 1966.

4. T. P. Liddiard, Jr. and D. Price, "Recalibration of the Standard Card-Gap Test", NOLTR 65-43, 20 Aug 1965.

5. G. E. Hauver and A. Melani, "Shock Compression of Plexiglas and Polystyrene", BRL R-1259, Aug 1964.

6. J. O. Erkman, "Behavior of PMMA Cylinders Under Shock Loading by Pentolite Charges", NOLTR 70-265, 12 Apr 1971.

7. J. O. Erkman, "Velocity of Detonation From Camera Records", NOLTR 68-117, 19 Sep 1968.

8. D. J. Edwards, J. O. Erkman, and S. J. Jacobs, "The Electromagnetic Velocity Gage and Applications to the Measurement of Particle Velocity in PMMA", NOLTR 70-79, 20 Jul 1970.

9. R. J. Lawrence and D. S. Mason, "WONDY IV - A Computer Program for One-Dimensional Wave Propagation with Rezoning", SC-RR 710 284, Aug 1971.

10. M. Kamegai and J. O. Erkman, "Numerical Analysis of a Diverging Shock Wave in Plexiglas Cylinders", Proceedings, Fifth Symposium (International) on Detonation, ACR-184, Office of Naval Research, Arlington, Virginia, 1970.

11. D. J. Edwards, J. O. Erkman, and Donna Price, "The Measurement of Particle Velocity in Pressed Tetryl", NOLTR 72-83, 3 Aug 1972.

REFERENCES (Cont.)

12. Van Thiel, editor "Compendium of Shock Wave Data", Lawrence Radiation Laboratory, UCRL-50108, 1966.

13. W. E. Deal, "Shock Wave Research on Inert Solids", Fourth Symposium on Detonation, ACR-126, Office of Naval Research, Washington, DC., 1965.

14. L. M. Barker and R. E. Hollenbach, "Shock Wave Studies of PMMA, Fused Silica and Sapphire", J. Appl. Physics 41 (10), 4208 (1970).

15. K. W. Schuler and J. W. Nunziato, "The Dynamic Mechanical Behavior of Polymethyl Methacrylate", The Sixth International Congress of Rheology, Lyons, France, 1972.

16. D. R. Christman, "Dynamic Properties of Poly(Methylmethacrylate) (PMMA) (Plexiglas)", DNA 2810 F (MSL-71-24), Mar 1972.

17. D. N. Schmidt and M. W. Evans, Nature 206, 1348 (1965).

18. N. L. Coleburn, "The Dynamic Compressibility of Solids from Single Experiments Using Light-Reflecting Techniques", NAVWEPS 6026, January 1961.

# APPENDIX A

## ESTIMATION OF ERRORS FOR MEASUREMENT OF PARTICLE VELOCITY WITH THE ELECTROMAGNETIC GAGE

The basic equation for the electromagnetic gage is

$$u = 10^4 \, v/H\ell \tag{A1}$$

where u is the particle velocity (mm/μsec), v is the output of the gage (volts), H is the magnetic field strength (gauss) and $\ell$ is the length of the base of the gage (mm). The quantity $\ell$ is measured directly with a micrometer so that an estimate of error is straightforward. H is measured with a gaussmeter prior to the shot as will be described later. The quantity v is measured indirectly and can be in error because of several sources. It is measured by using an oscilloscope which must be calibrated before each shot. A reference line is placed on the film by triggering the scope manually, see Figure A1. A voltage, E, is then applied to the input to the scope and it is manually triggered again, giving reference line 2. Then the experiment is performed, giving a trace -- see Figure A1 for an illustrative example. When the film record is read, the separation of the two reference lines is measured. Call this distance x as shown in the figure. Next, the trace is read; this amounts to measuring the vertical distance from the base line -- the dashed line in Figure A1 -- to a point on the trace. For a particular point on the trace, call this displacement y. We assume that the scope is linear so that displacement of the trace is proportional to the voltage, or

$$v_1 = E \, y \, / x. \tag{A2}$$

The voltage $v_1$ is not that generated by the gage; it is the output of the circuit shown in Figure A2. The foil is represented as a voltage generator having negligible resistance with a resistance r in series. The reason for incorporating this resistance is given elsewhere. The load resistor, R, is that of the terminating resistor at the oscilloscope. From the diagram it is evident that

$$v = v_1 \, (R + r) \, / R \qquad = E \, y \, (R + r) \, / \, x \, R \tag{A3}$$

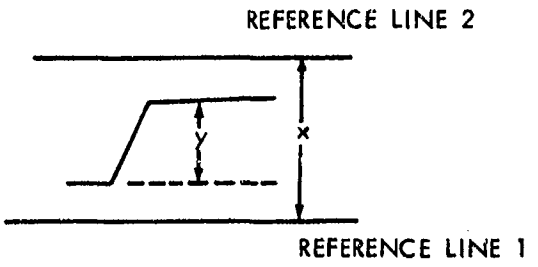


FIG. A1 IDEALIZED OSCILLOSCOPE RECORD

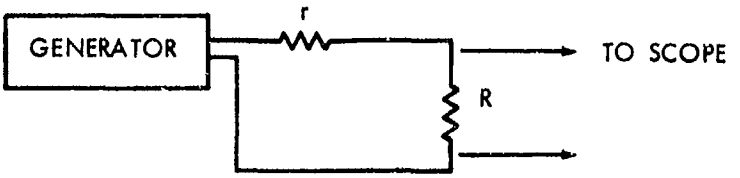


FIG. A2 CIRCUIT OF EMV GAGE

Thus the particle velocity is given by

$$u = 10^4 \, E \, y \, (R + r)/(H\ell \times R). \qquad (A4)$$

In order to estimate the error in u, Equation (A4) is differentiated logarithmetically, giving

$$\frac{\Delta u}{u} = \frac{\Delta \ell}{\ell} + \frac{\Delta E}{E} + \frac{\Delta x}{x} + \frac{\Delta y}{y} + \frac{(\Delta R+\Delta r)}{(R+r)} + \frac{\Delta R}{R} + \frac{\Delta H}{H} \qquad (A5)$$

where all negative signs have been changed to positive. We must estimate the uncertainty in each quantity, $\Delta E$, $\Delta \ell$, etc., so that their cumulative effect on the particle velocity can be calculated. This is the simplest way to estimate the error. A more sophisticated method (which gives more optimistic results) is to compute $\Delta u/u$ by taking the root mean square of the values of the terms on the right hand side of Equation (A5). Note that the result will be a relative value, a nondimensional number. It will be more convenient to deal with percentages in the following so that each side of Equation (A5) is multiplied by 100%.

The first term involves $\ell$, the length of the base of the EMV gage. For most of our work, this length is determined by the thickness of a piece of PMMA or explosive around which the foil is wrapped part way. The thickness of the test material varies from 2.5 to 10.0 mm and is measured using a micrometer. Assuming these measurements are accurate to ±0.013 mm (0.0005 inch), the accuracy is ±0.48% for the short pickup and ±0.12% for the longest pickup. The reason for using short pickups is to minimize the effects of curvature on the rise time of the signal. That is, when we place a gage within 50 mm of the point of initiation of an explosive, we use a short pickup. Some of our close-in measurements may be in error due to the inaccurate measurements of the base length of the gage. Note, however, under these circumstances, the particle velocity is large, so that other sources of errors are at their minimum.

The next term, $\Delta E/E$, is the error in measuring the voltage applied to the scope for calibration. This voltage is supplied by a small DC power supply. It is measured with a Model 7050 Fairchild digital multimeter. For temperatures between 15 and 35°C, the accuracy of the multimeter is claimed to be ±0.1% of the reading, ±1 digit. We use the 1.5 volt scale so that one digit is $10^{-3}$ volts. Thus the % error is $\pm 0.1(1.0 + E) / E$; this function is plotted in Figure A3. Our estimated error obviously becomes more troublesome when we have to measure small voltages. Our lowest voltage is about 0.15 volts for which we can expect an error of about 1%. The error due to this

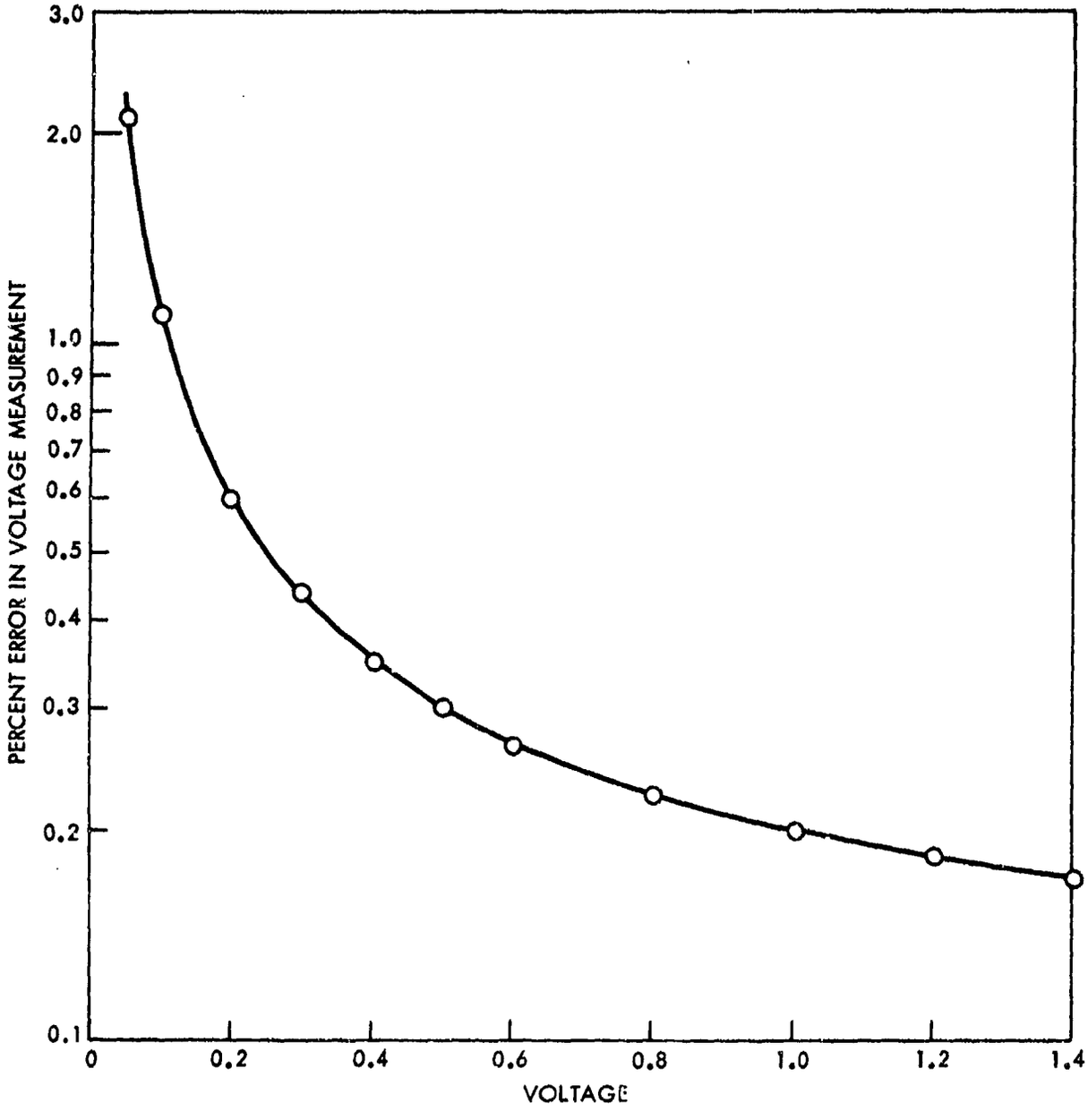


FIG. A3 ERROR IN READING THE DIGITAL MULTIMETER

source is the same for all points read off any one record. It will differ, of course, from one record to the next to the extent to which we change the calibrating voltage.

The quantity, x, is a measure of the displacement of the oscilloscope beam due to the calibrating voltage, E. This displacement is read with a Universal Telereader. It is doubtful if the measuring instrument is limiting our accuracy in this case. Rather, our accuracy is limited by the ability of the operator to place a crosswire accurately on the image of the trace. These traces, which are placed on the film prior to a shot, are usually narrow and distinct and are therefore relatively easy to measure. The operator claims that a reading can be repeated to within ±10 counts. The distance being measured on the film is usually about 20 mm, or 1600 counts on the Telereader. If both lines are read to the same precision, this distance is uncertain to ±20 counts, or 1.25%. This error is the same for any one record. It does not change much from record to record even though the particle velocity may vary by a factor of 20. This is due to the fact that we change the gain of the amplifiers of the scope to give about 20 mm displacement each time we calibrate the scope. We assume, of course, that the amplifiers are linear.

The next term involves y, the quantity which represents the displacement of a point on the dynamic record from the base line, see Figure A1. In the usual case, we measure a displacement of about 10 mm on the film, or about 800 counts on the Telereader scale. Again we assume that the Telereader is so accurate that it does not limit our accuracy. The crosswires can be reset on a trace, and on the baseline, to within about ±10 counts. Thus the displacement of the trace is uncertain to ±20 counts, or about 2.6%. As in the case of the measurement of x as discussed above, the error due to the measurement of y does not change from record to record. The reason is the same, we change the amplification of the scope so that the trace is displaced about the same in each shot. Because we are usually measuring a decaying signal, the error does change some over each individual trace.

Reported results never depend on the reading of a single point on the trace of a record. Many points are read so that a plot of u vs time can be constructed. A subset of the points may be fitted to a straight line so that the value of u can be obtained at zero time (an extrapolation back through the rise time of the signal). In other cases, lines are drawn through the data to locate more or less distinct changes of slope of the trace. This graphical treatment has been used to determine the Chapman-Jouguet particle velocity and the reaction time in explosives. Analysis of the errors under these more complicated circumstances has not been made. The error reported here applies to the reading of only a single point on the trace of an oscilloscope record.

We use a Rawson-Lush Model 824 rotating coil gaussmeter to measure the field, H. The accuracy of this instrument is 0.1% or 0.5 gauss, whichever is larger. We work with fields whose strength vary from

400 to 1000 gausses, so that our accuracy varies from 0.12% to 0.1%. Errors of this magnitude are negligible. Our method of operation may introduce other errors in the field, however. The magnet is energized and the field is measured before the experiment is completely assembled. The current to the magnet is measured on a 0-50 ampere ammeter calibrated to 0.25% of full scale. The current is then reduced to zero, the leads to the magnet are disconnected for reasons of safety, and the experiment including the explosive, is put into place. Immediately before firing, the current to the magnet is restored to the same value as before. Firing takes place within 3 to 5 minutes of the time that the current is restored. Drift in the output of the power supply during this short time is negligible.* If the magnet assembly was not disturbed during the final assembly of the experiment, and if the ammeter readings were the same, we should have the same field as that during the measurement with the gaussmeter. Reading the ammeter may introduce an error in the field strength. The meter has a mirror scale which helps eliminate parallax during reading. On repeated trials to check on this possibility, the field is returned to within 1.0 gauss of the original reading. This gives an error of 0.25% at 400 gauss and 0.1% at 1000 gauss. We hope that in routine operation that we do this well.

Both of the resistors in the circuit, see Figure A1, have nominal values of 50 ohms. They are used to terminate the signal cable so that the reflection of electrical signals will be minimized. The precision of the resistor, R, which is located at the oscilloscope, is ±0.5%. Hence the value of $\Delta R/R$ is also ±0.5%. The resistor, r, is an inexpensive carbon resistor which is destroyed in the experiment. Its resistance is measured on a bridge to a precision of ±0.25% prior to assemblying the shot. Converting the percentages given above to increments of resistances gives 0.38% for the term $(\Delta R + \Delta r)/(R + r)$. Hence we have a total error from the resistors of 0.88%. This value can be reduced by a careful measurement of the resistance at the oscilloscope (resistor R). Note that in the above that the resistance of the cable has been neglected.

The errors are summarized below for three values of u. This illustrates how the error in the three digit voltmeter changes the error as u is changed. The error in y is included in the table so that the results do not apply, for example, to the determination of a peak value of u which usually depends on fitting many values of u to a function for extrapolation to zero time.

In the analysis of error given above, we assumed that experimental arrangements were reproducible. There may be variations in the

---

*The power supply is an Electronic Measurements Model SCR 120-20, three phase, constant current instrument.

SUMMARY OF ERRORS

| u, mm/μsec | 2.0 | 1.0 | 0.1 |
|---|---|---|---|
| $\Delta\ell/\ell$ | 0.50 | 0.5 | 0.5 |
| $\Delta E/E$ | 0.14 | 0.24 | 0.75 |
| $\Delta x/x$ | 1.26 | 1.26 | 1.26 |
| $\Delta y/y$ | 2.6 | 2.6 | 2.6 |
| $(\Delta R+\Delta r)/(R+r)$ | 0.38 | 0.38 | 0.38 |
| $\Delta R/R$ | 0.5 | 0.5 | 0.5 |
| $\Delta H/H$ | 0.25 | 0.25 | 0.25 |
| Sum of Errors | 5.63 | 5.73 | 6.24 |

density of the PMMA from sample to sample. The same is true of the pentolite pellets. The PMMA samples are machined in a lathe so that they are at least in the correct geometrical shape. The pressed pentolite pellets are somewhat barrel shaped -- the diameters of the midplane of the pellets are about 0.003 inch greater than the diameter of their faces. The faces are bulged so that on the axis the pellets are 0.005 to 0.006 inch thicker than they are at their edges. Thus when two pellets are stacked, it is possible to have a gap 0.012 inch thick over part of the area between them. This interferes with the transfer of detonation from one pellet to another, introduces a tilt in the detonation wave, and distorts the Taylor wave. At the explosive/PMMA interface, the gap may be 0.006 inch over part of the surface (assuming the PMMA is flat on the end). Again this introduces tilt in the shock wave in the PMMA and distorts the rarefaction wave which follows the shock front.

The shape of tetryl pellets are closer to that of a cylinder. They may be as much as 0.002 inch thicker on their axes than at their edges. Their diameters may be 0.002 inch too great at their midplanes.

Our calibration work might have been easier if we had machined the pressed pellets into true cylindrical forms. Then, however, the calibration would not have corresponded to the actual situation in the gap test.